PB83-261768

Chemistry, Physics, and Optical Properties of Plumes and Background Air in the Southwest United States

Sonoma Technology, Inc., Santa Rosa, CA

Prepared for

Environmental Sciences Research Lab.
Research Triangle Park, NC

Sep 83

U.S. Department of Commerce
National Technical Information Service
NTIS

EPA-600/3-83-085
September 1983

THE CHEMISTRY, PHYSICS, AND OPTICAL PROPERTIES OF PLUMES AND BACKGROUND AIR IN THE SOUTHWEST UNITED STATES

PB83-261768

Project Coordinator

D.L. Blumenthal
Meteorology Research, Inc.
Santa Rosa, California 95401
Current Address: Sanoma Technology, Inc., Santa Rosa, California

Task Managers

L.W. Richards
Meteorology Research, Inc.
Santa Rosa, California 95401
Current Address: Sanoma Technology, Inc., Santa Rosa, California

E.S. Macias
Department of Chemistry, Washington University
St. Louis, Missouri 63130

R.W. Bergstrom
Systems Applications, Inc.
San Rafael, California 94903

Project Coordinator for Salt River Project

P.S. Bhardwaja
Salt River Project
Phoenix, Arizona 85001

Contract 68-02-3225

Project Officers

William E. Wilson, Jr., and William D. Conner
Environmental Sciences Research Laboratory
Research Triangle Park, North Carolina 27711

ENVIRONMENTAL SCIENCES RESEARCH LABORATORY
OFFICE OF RESEARCH AND DEVELOPMENT
U.S. ENVIRONMENTAL PROTECTION AGENCY
RESEARCH TRIANGLE PARK, NORTH CAROLINA 27711

REPRODUCED BY
NATIONAL TECHNICAL
INFORMATION SERVICE
U.S. DEPARTMENT OF COMMERCE
SPRINGFIELD, VA. 22161

TECHNICAL REPORT DATA
(Please read Instructions on the reverse before completing)

1. REPORT NO. EPA-600/3-83-085	2.
3. RECIPIENT'S ACCESSION NO. PB83 261768	
4. TITLE AND SUBTITLE THE CHEMISTRY, PHYSICS, AND OPTICAL PROPERTIES OF PLUMES AND BACKGROUND AIR IN THE SOUTHWEST UNITED STATES	5. REPORT DATE September 1983
	6. PERFORMING ORGANIZATION CODE
7. AUTHOR(S) D.L. Blumenthal, et al.	8. PERFORMING ORGANIZATION REPORT NO.
9. PERFORMING ORGANIZATION NAME AND ADDRESS Sanoma Technology, Inc. Santa Rosa, CA 95401	10. PROGRAM ELEMENT NO. CDTA1D/11-0543 (FY-83)
	11. CONTRACT/GRANT NO. 68-02-3225
12. SPONSORING AGENCY NAME AND ADDRESS Environmental Sciences Reseach Laboratory - RTP, N.C. Office of Research and Development U.S. Environmental Protection Agency Research Triangle Park, North Carolina 27711	13. TYPE OF REPORT AND PERIOD COVERED Interim 5/4/79 to 11/1/81
	14. SPONSORING AGENCY CODE EPA/600/09
15. SUPPLEMENTARY NOTES	

16. ABSTRACT

VISTTA (Visibility Impairment due to Sulfur Transport and Transformation in the Atmosphere) is a cooperative program involving numerous government agencies, private companies, and universities and is jointly sponsored by the U.S. Environmental Protection Agency and Salt River Project. During the summer and winter of 1979, plume measurement programs were conducted near the Navajo Generating Station (NGS), at Page, Arizona. Results indicated that: (1) For the NGS plume, under most lighting and viewing conditions, NO_2 dominates the blue light extinction and brown coloration due to the plume. (2) Widespread areas of elevated aerosol concentartions were documented in the Southwest due to long range transport from the Southern California area and wildfires. Other causes of regional haze are known to exist but were not documented in this study. (3) Evaluation of the chemistry, aerosol growth, and optics components of the PLUVUE plume visibility model showed predictions to be in reasonable agreement with the measurements. More uncertainty was encountered with the diffusion component. A set of nine reactions among NO, NO_2, O_3, O_2, SO_2, OH, H_2O, and $O(^1D)$ was found to adequately simulate the plume chemistry for the clean dry background conditions at NGS.

17. KEY WORDS AND DOCUMENT ANALYSIS

a. DESCRIPTORS	b. IDENTIFIERS/OPEN ENDED TERMS	c. COSATI Field/Group

18. DISTRIBUTION STATEMENT RELEASE TO PUBLIC	19. SECURITY CLASS (This Report) UNCLASSIFIED	21. NO. OF PAGES 77
	20. SECURITY CLASS (This page) UNCLASSIFIED	22. PRICE

EPA Form 2220-1 (Rev. 4-77) PREVIOUS EDITION IS OBSOLETE

DISCLAIMER

This report has been reviewed by the Office of Research and Development, U.S. Environmental Protection Agency, and approved for publication. Mention of trade names or commercial products does not constitute endorsement or recommendation for use.

ABSTRACT

VISTTA (Visibility Impairment due to Sulfur Transport and Transformation in the Atmosphere) is a cooperative program involving numerous government agencies, private companies, and universities and is jointly sponsored by the U.S. Environmental Protection Agency and Salt River Project. During the summer and winter of 1979, plume measurement programs were conducted near the Navajo Generating Station (NGS), at Page, Arizona.

During VISTTA, ground and airborne measurements of aerosol size distribution, chemistry and optical properties, as well as trace gas concentrations; were made in the plume and in background air. Extensive regional and plume telephotometer measurements, airborne measurements along telephotometer sight paths, background meteorological measurements, and source aerosol and chemistry measurements were also made. Various types of visibility measurements were compared with one another and with calculations of light extinction made using aerosol and NO_2 data. The measured plume optical effects were compared to those predicted using the EPA-SAI plume visibility model (PLUVUE).

The data base collected during VISTTA can be used for plume visibility model evaluation. Specific data from 27 sight paths through the NGS plume on June 28, July 13, December 4, 7, and 15 have been tabulated and are available for model evaluation. These data include:

- Emission characteristics of the NGS.
- Meteorological data and sun-observer-plume geometry.
- Background trace gas, aerosol, and visibility data.
- Telephotometer measurements of the plume made from four sites.
- Aircraft measurements made along the telephotometer sight path, which include plume width, pollutant concentrations, and particle light scattering (b_{sp}).

The results of the study to date indicate that:

- For the NGS plume, under most lighting and viewing conditions, NO_2 dominates the blue light extinction and brown coloration due to the plume.

- For distances up to 100 km or more for power plants like NGS, secondary aerosol formation can be ignored in visibility models under the dry conditions studied.

- Widespread areas of elevated aerosol concentrations were documented in the Southwest due to long range transport from the Southern California area and wildfires. Other causes of regional haze are known to exist but were not documented in this study.

- Evaluation of the chemistry, aerosol growth, and optics components of the PLUVUE plume visibility model showed predictions to be in reasonable agreement with the measurements. More uncertainty was encountered with the diffusion component. A set of nine reactions among NO, NO_2, O_3, O_2, SO_2, OH, H_2O, and O('D) was found to adequately simulate the plume chemistry for the clean dry background conditions at NGS.

CONTENTS

Abstract iii
Figures. vii
Tables viii
Acknowledgments. ix

1. Introduction and Objectives. 1
2. Conclusions. 4
3. Project Summary. 7
   3.1 Location and Meteorology. 7
      3.1.1 Navajo Generating Station. 7
      3.1.2 Ground and Airborne Measurements 9
      3.1.3 Meteorology. 9
   3.2 VISTTA Measurement Program. 10
      3.2.1 Experiment Design. 10
      3.2.2 Measurement Systems. 11
      3.2.3 NGS Emissions. 14
      3.2.4 Plume Chemistry and Aerosol Physics. 16
         3.2.4.1 Nitrogen Chemistry. 16
         3.2.4.2 Sulfur Chemistry. 17
         3.2.4.3 Secondary Aerosol Formation 18
      3.2.5 Plume Optics 19
      3.2.6 Background Aerosol Composition and Contributions to Regional Haze in VISTTA Study Area. 20
      3.2.7 Regional Haze - Transport and Distribution 23
         3.2.7.1 Transport from Southern California June 29-30, 1979. 23
         3.2.7.2 Forest Fire Plumes: July 4-5, 1979 24
         3.2.7.3 Other Days. 24
         3.2.7.4 Bryce Canyon-Zilnez Mesa Comparison 24
   3.3 Model Evaluation. 25
      3.3.1 Dispersion Module. 25
      3.3.2 Chemistry and Aerosol Module 25
      3.3.3 Optics Module. 26
      3.3.4 Overall Model Evaluation 26

3.4 Methods Comparisons 27
3.4.1 Telephotometers Comparisons. 27
3.4.2 Telephotometers-Nephelometer Comparisons 27
3.4.3 Sulfur Measurements. 28
3.5 Discussion. 28
4. Case Studies for Plume Visibility Model Evaluation 31
4.1 Case Study Introduction 31
4.2 Description of the Data Base for Plume Visibility Model Evaluation. 33
4.2.1 Plume-Sun-Observer Geometry. 35
4.2.2 Emission Data. 35
4.2.2.1 Flue Gas Characteristics. 35
4.2.2.2 Emission Rates of Primary Pollutants. . . . 43
4.2.3 Meteorological Data. 43
4.2.3.1 Wind Speed. 43
4.2.3.2 Wind Direction. 44
4.2.3.3 Temperature 44
4.2.3.4 Relative Humidity 45
4.2.4 Background Data. 45
4.2.4.1 Trace Gas 45
4.2.4.2 Aerosol Data. 46
4.2.4.3 Nephelometer Measurements 46
4.2.5 Measurements of Plume Characteristics. 47
4.2.5.1 Plume Visual Effects--Ground-Based Measurements. 47
4.2.5.2 Aircraft Measurements of the Plume. 47
4.2.6 Additional Data for Optics Component Evaluation. . . 47
4.3 Data Base for Plume Visibility Model Evaluation 49

References. 63

FIGURES

Number		Page
1	Map of the VISTTA study areas.	3
2	Detail map of the study area	8
3	Case studies: June 28, 1979	36
4	Case studies: July 13, 1979	37
5	Case studies: December 4, 1979.	38
6	Case studies: Morning of December 7, 1979	39
7	Case studies: Afternoon of December 7, 1979	40
8	Case studies: December 15, 1979	41
9	Schematic representation of sun-plume-observer geometry.	48
10	Case studies for plume visibility model evaluation	55
11	Temperature profile for the case study of June 28, 1979 at 0900 MST	56
12	Temperature profile for the case study of July 13, 1979 at 0500 and 0900 MST.	57
13	Temperature profile for the case study of December 4, 1979 at 0856 MST	58
14	Temperature profile for the case study of December 7, 1979 at 0847 MST	59
15	Temperature profile for the case study of December 7, 1979 at 1248 MST	60
16	Temperature profile for the case study of December 15, 1979 at 0845 MST	61

TABLES

Number		Page
1	Measurements Made on MRI Queen Air and EPA/LV.	12
2	Measurements Made at Zilnez Mesa and Copper Mine Site.	13
3	Measurements Made at Page Site	14
4	Summary of Average NGS Emission Rates July 1-July 10, 1979	15
5	Plume Intensity/Sky Intensity.	20
6	Chemical Species Mass and Extinction Balance for Zilnez Mesa	22
7	Program Activities	32
8	Instrumentation Used in VISTTA Measurements.	42
9	Emission Rates for the Navajo Generating Station Field Program--1979.	44
10	Pasquill Stability Class	45
11	Summary of Kinds of Data Collected During the EPA/VISTTA 1979 Field Programs.	50
12	Data Common to All Case Studies.	51
13	1979 VISTTA Case Studies	53

ACKNOWLEDGMENTS

This work has been supported as part of the VISTTA project by the Federal Interagency Energy/Environment Research and Development Program through a contract with the EPA ESRL Office of Regional Studies. We are grateful to William Wilson, EPA Project Officer, for his active participation in and support of this work. VISTTA is cosponsored by the Salt River Project, whose cooperation and participation has contributed significantly to the study. Ten other organizations participated in VISTTA either as subcontractors or under grants from the EPA, and provided the range of capabilities required for a program of this scope.

SECTION 1

INTRODUCTION AND OBJECTIVES

In 1977, the U.S. Congress amended the Clean Air Act to set as a national goal the "prevention of any future, and the remedying of any existing, impairment of visibility in mandatory class I Federal areas which impairment results from man-made pollution" (Section 169A). In order to accomplish this goal, an understanding of the effects of current and proposed emissions on visibility is necessary. In the southwestern U.S., visibility impairment is believed to be caused in large part by sulfur-emitting sources such as urban areas, smelters, and power plants. The percentage of the total sulfur emissions due to power plants is expected to increase in future years as more coal-fired plants are built and as sulfur emissions from smelters are further reduced by new controls. To develop the technical information required to understand the contribution of coal-fired power plants to visibility impairment in western pristine areas, the U.S. Environmental Protection Agency (EPA) initiated the VISTTA project (Visibility Impairment due to Sulfur Transport and Transformation in the Atmosphere).

The VISTTA project is a multiyear cooperative effort involving several government agencies, private companies, and universities, with the overall coordination of the program the responsibility of Meteorology Research, Inc. (MRI).*

The general goals of the VISTTA project are to:

- Determine the relationship between emissions of coal-fired power plants and their downwind optical effects.
- Document the current natural and anthropogenic contributors to visibility impairment in the southwestern U.S. and the relative contribution of the various sources, so that the contribution of power plants to the total can be determined.
- Provide data for evaluation of plume visibility models.

*In October 1982 this responsibility was transferred, along with the project scientists involved, to Sonoma Technology Inc., Santa Rosa, California.

During the summers of 1977 and 1978, preliminary VISTTA experiments were performed using an instrumented aircraft to measure chemical and physical properties of selected point source plumes as well as regional haze in the southwestern U.S.

In 1979, two major field studies were conducted at and around the Navajo Generating Station (NGS) at Page, Arizona--one from June 26 to July 14 and the second from December 1 to 16 (Figure 1). The specific objectives of the 1979 studies were to:

> Measure the chemical, optical, and physical properties of the NGS plume.

> Characterize the regional background aerosol and chemical environment near the power plant.

> Estimate the contributions of various sources to the regional haze using chemical element balance and extinction budget techniques.

> Analyze background and plume data to determine the effects of various plume components on plume optical effects and to evaluate EPA's PLUVUE visibility model.

This report summarizes the measurements and results to date of the June-July and December 1979 plume studies and model evaluations.*

Section 2 of this report presents the conclusions from the 1979 measurements and model evaluations. Section 3 summarizes the measurements made and the results of the data analyses and model evaluations. Section 4 presents cases of specific data that are characteristic of the NGS plume and surrounding region. These data may be used to evaluate visibility models.

---

*Participants in the 1979 studies: Meteorology Research, Inc. (MRI); Systems Applications, Inc. (SAI); Washington University (WU); University of Minnesota (UM); University of Washington (UW); University of California at Los Angeles (UCLA); Washington State University (WSU); University of Vienna (UV); Harvey Mudd College (HMC); University of California at Davis (UCD); EPA-Las Vegas (EPA/LV); and Salt River Project (SRP).

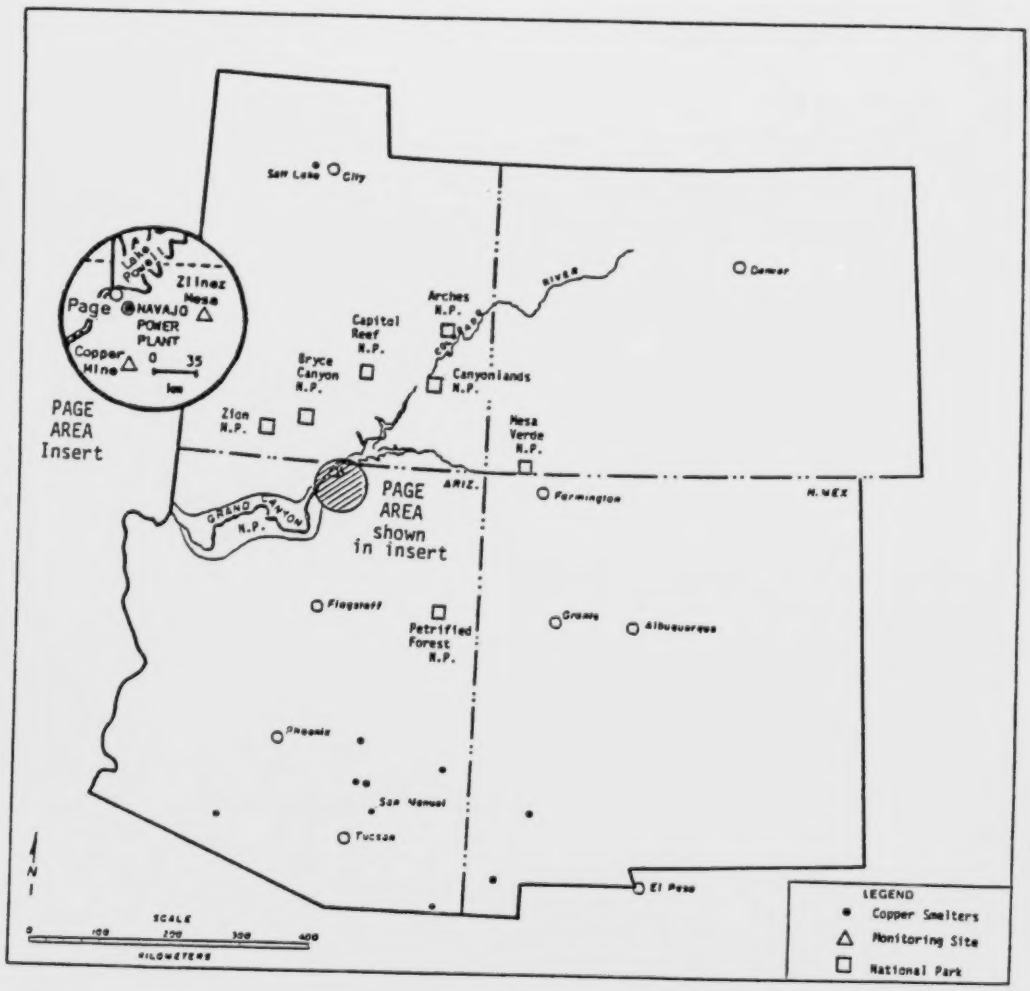

Figure 1. Map of the VISTTA study area.

SECTION 2

CONCLUSIONS

> For the NGS plume, under most lighting and viewing conditions within 50 km of the plant, NO_2 dominates the blue light extinction and brown coloration due to the plume. At distances less than 10 km, primary particles greater than 1 μm in diameter can dominate the light extinction at all visible wavelengths. The primary particle size distribution in the plume near the source has a small maximum under 0.1 μm diameter and a dominant maximum near 3.5 μm diameter. For modeling purposes, a mass median diameter of 3.5 μm should be used for NGS emissions.

> Sulfate formation rates in the NGS plume in both summer and winter under dry conditions were between 0 and 1% per hour. The NO_2 to HNO_3 conversion rate was substantially more rapid than the SO_2 to sulfate conversion rate, but the nitric acid remained in the gaseous state. The sulfate formed was largely ammonium sulfate. No particulate nitrates were measured in the plume. At distances up to 100 km in the plume, particle formation and growth were only detected in the size range below 0.1 μm and resulted in insignificant optical effects compared to those due to the background aerosol. Some aerosol was probably formed in particles larger than 0.1 μm, but this formation was obscured by variations in the background aerosol concentration. Gas-to-particle conversion was undetectable at night and while SO_2 concentrations were greater than about 100 ppb.

> The greatest causes of visibility impairment in the region during the 1979 summer study were widespread areas of elevated aerosol concentrations at different times due to:

1. Long-range transport from the Southern California area 800 km away, and

2. Wildfires.

> Although shown to be important by other studies, significant regional visibility impairment due to smelters or soil-derived elements (windblown dust) was not measured during the short 1979 summer VISTTA study.

> During this study, visibility impairment was generally caused by nonsoil aerosol. On hazy days, sulfates and organic carbon compounds dominated the fine particle aerosol composition. Fine particle chemical species contributed to light extinction approximately in proportion to their contribution to aerosol mass.

> Visibility reduction due to regional haze can equal or exceed the reduction caused by a plume from a nearby well-controlled power plant.

> In the NGS plume, NO_2 from primary emissions and the termolecular reaction can account for 3% to 6% of the measured NO_x near the source. For a given total amount of NO_x in any plume cross section, the NO_2 concentrations can be adequately modeled by assuming the photostationary-state relationship of NO, O_3, and NO_2. For dilute southwestern plumes (<100 ppb SO_2 at NGS), the reaction of NO_2 with OH represents a significant NO_2 loss mechanism, which should be accounted for in models.

> Evaluation of the chemistry, aerosol growth, and optics components of the EPA visibility model (PLUVUE) showed predictions to be in reasonable agreement with the measurements. More uncertainty was encountered with the dispersion component. The nine reactions used in PLUVUE adequately model the plume chemistry measured at NGS. For visibility modeling at power plants like NGS, for distances up to 100 km, secondary aerosol formation can be ignored under clean, dry conditions.

> Comparisons between ground-based contrast telephotometer and Integrating Nephelometer data obtained during the program showed good agreement on days of regional homogeneity. The choice of targets was found to be important; the best correlations ($r > 0.9$) were for targets to the north. Inherent contrast changes in the targets with sun angle can substantially vary the correlation.

> Good agreement was found between the extinction coefficients determined by an Integrating Nephelometer on a background sight path flight and the telephotometer viewing along the same sight path.

> Comparison and calibration of 12 multiwavelength contrast telephotometers showed an inherent error of about 1% or less in the

contrast (ratio) mode and about 10% in the absolute radiance mode. Operator differences can increase the variation in contrast mode to 2% with a resulting variation in the calculated extinction coefficient of up to 15%.

> The SO_2 emission rate per BTU from NGS was found to typically vary less than 15%. Emission rates of NO_x and particulate matter per BTU, on the other hand, varied by about a factor of 2, complicating the prediction of visual impact in the definable plume.

> The chemical composition of the southwestern aerosol is substantially different for aerosol above and below about 1 μm diameter. For optimum separation of the coarse and fine aerosol, size-segregating samplers used in the southwestern U.S. should have a cut point near 1 μm diameter.

> The following findings suggest that NO_x and its oxidation products will be removed from the atmosphere more rapidly than SO_2 and its oxidation products, with the result that NO_x emissions have an impact over a smaller region than SO_2 emissions: (1) NO_x is oxidized to nitric acid (gas) several times more rapidly than SO_2 is oxidized to sulfate (particles); (2) gases are removed from the atmosphere more rapidly than particles; and (3) the air masses transported from Southern California contained easily measurable sulfate concentrations, but the nitrate concentrations were near the detection limit.

> The June-July and December 1979 VISTTA field programs provided an extensive data base for the evaluation of plume visibility models and of their individual components (e.g., dispersion, chemistry, and optics components). It is important to note, however, that the performance of a plume visibility model can vary according to the conditions considered. The VISTTA case studies presented in this report were obtained for a specific set of conditions (i.e., a power plant plume with particulate emission control in a relatively clean and dry atmospheric environment at downwind distances of less than 35 km). Further evaluation of plume visibility models would require the development of other data bases.

SECTION 3

PROJECT SUMMARY

Prepared by:

D. L. Blumenthal*, L. W. Richards*, and S. L. Eigstit
Meteorology Research, Inc.

E. S. Macias
Washington University

R. W. Bergstrom
Systems Applications, Inc.

P. S. Bhardwaja
Salt River Project

W. E. Wilson
Environmental Protection Agency

3.1 LOCATION AND METEOROLOGY

3.1.1 Navajo Generating Station

The Navajo Generating Station was selected for this study because it is an example of a new stationary source located in a remote desert area of the Southwest. It is a large coal-fired power plant consisting of three 750 MW (net) units using three stacks, each 235 meters tall. Particulate emissions are controlled with electrostatic precipitators with a design efficiency of 99.5%. Sulfur dioxide emissions are controlled by the use of low-sulfur coal; the plant does not have scrubbers for the removal of sulfur dioxide. The plant is isolated from other sulfur dioxide sources and is in the vicinity of several mandatory class I Federal areas. The location of the plant is shown in Figure 2. The power plant is in high desert terrain (elevation 1325 m msl) in a region of generally good visibility, averaging about 110 km (Bhardwaja et al., 1981).

---

* Current Affiliation: Sonoma Technology, Inc., Santa Rosa, CA.
† Current Affiliation: Qume Corp., San Jose, CA.

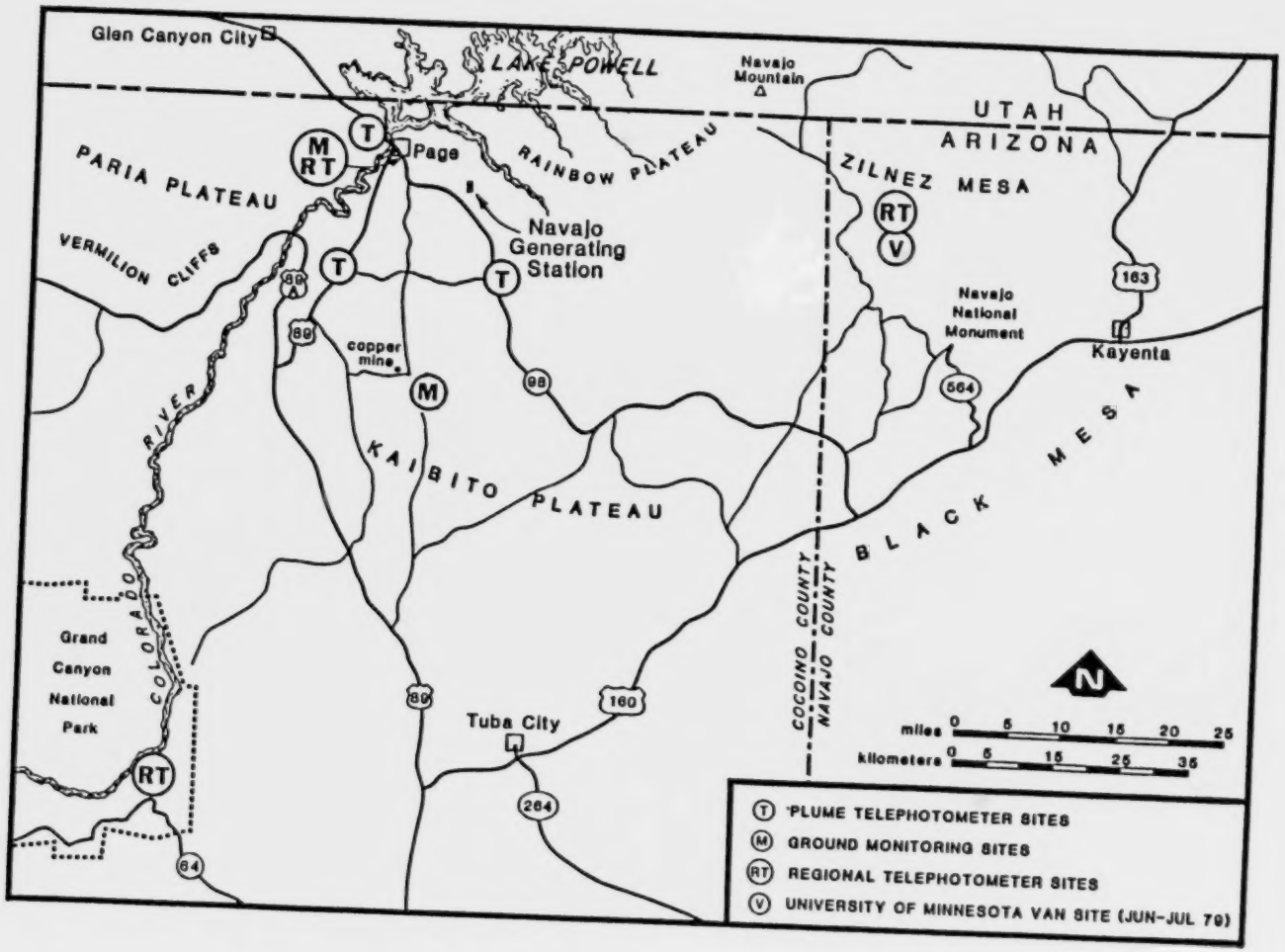

Figure 2. Detail map of the study area.

3.1.2 Ground and Airborne Measurements

Surface-based aerosol and atmospheric chemistry measurements were made at three sites. During the summer study, measurements were made at Page (elevation 1310 m msl), at Zilnez Mesa (elevation 2290 m msl), and at Copper Mine (elevation 1925 m msl) (Figure 2). In the winter study, only the Page and Copper Mine sites were used. The Page site was in a sparsely populated area at the edge of town. The other two sites were at remote microwave towers and were chosen because they were likely to be impacted by the plume during the study, but only one at a time with the other serving as a background site. These two sites were both in extremely remote areas with almost no vehicular traffic passing the sites. The Zilnez Mesa site had a clear view of the plant.

During the summer study, regional as well as plume aircraft measurements were made. These flights covered a region extending from Farmington, New Mexico, on the east, to Las Vegas, Nevada, on the west, and from near Salt Lake City, Utah, on the north, to Phoenix, Arizona, on the south.

Telephotometer measurements of the NGS plume were made from numerous locations within about 50 km of the plant. In addition, regional telephotometer and nephelometer data were obtained at Zilnez Mesa, Page, and Copper Mine as part of the VISTTA program or from an EPA network at Bryce Canyon, Canyonlands, and Grand Canyon National Parks (see Babson et al., 1982).

3.1.3 Meteorology

Both the summer and winter study periods were characterized by clear, dry, sunny days and strong radiation inversions at night. For both the summer and winter periods, the temperature at 600 m above ground level (agl) at 0500 MST averaged 1.8^{o}C warmer than the surface. The plume was typically trapped in stable air at 600-700 m agl during the early morning hours. By midday in the summer, the lapse rate was generally adiabatic with good mixing to 1500 m agl or higher. During the winter period, a stable lapse rate usually prevailed all day. The temperature at 600 m agl at 1300 MST in the summer averaged 7.0^{o}C cooler than the surface temperature and only 3.2^{o}C cooler in the winter. The mean 1300 MST surface temperature was 33.8^{o}C during the summer period and 7.0^{o}C during the winter. Both summer and winter periods were very dry with a mean 1300 MST surface dew point of 1.1^{o}C in the summer and -6.7^{o}C in the winter.

3.2 VISTTA MEASUREMENT PROGRAM

3.2.1 Experiment Design

During the 1979 field projects, ground and airborne measurements of aerosol size distribution, chemical and optical properties, as well as gaseous reactant concentrations, were made in both the NGS plume and background atmosphere. In-stack size distribution and aerosol chemistry measurements were made to characterize the emissions. Extensive regional and plume telephotometer measurements, airborne measurements along telephotometer sight paths, and meteorological data were collected.

The following types of specific experiments were performed:

- Plume chemistry flights (see Section 3.2.4). Sampling flights were made during which plume samples were collected for later chemical analysis. These flights consisted of a series of orbits (approximately one hour each) at fixed locations in the plume and in background air with one set of grab samples (filters, impactors, etc.) collected during each orbit. Plume samples were usually collected at two or three distances from the plant, ranging up to 100 km downwind.

- Telephotometer sight path measurements (see Section 3.2.5 and Section 4 of this report for details). Sampling flights were made along numerous telephotometer sight paths both through the plume and through background air from the telephotometer to the target. Aerosol concentration and size distribution as well as gas concentrations were measured along the path.

- Regional flights (summer only; see Sections 3.2.6 and 3.2.7). Sampling flights were made by two aircraft to determine the composition and spatial variation of the regional haze. Aerosol size and chemistry as well as gaseous pollutants were measured. Regional flights were also made by one aircraft in the region upwind of Page on several days when the other aircraft was measuring plume chemistry.

- Ground based measurements of gases, aerosol chemistry and size distribution, and atmospheric optics (see Sections 3.2.6 and 3.2.7). These measurements were made continually throughout the field programs to document the temporal and spatial variations in the background conditions, and to occasionally document plume characteristics at ground level.

- Regional light extinction and scattering measurements (see Section 3.2.7). Telephotometer and Integrating Nephelometer data were obtained continuously from several sites throughout the sampling region. These instruments provided supporting measurements of the temporal and spatial variations in visibility and provided an opportunity for method comparisons.

- Method comparisons (see Section 3.4). Laboratory and field comparisons were performed between all the telephotometers used during the program, including commercial and research instruments, to compare the results from telephotometers and Integrating Nephelometers. Comparisons were made between extinction from telephotometer data and calculations of extinction made by integrating sight path aerosol data. Comparisons of several techniques for measuring sulfur aerosol and size distributions were made.

Throughout the program, all flights were supported by upper-air wind soundings every hour and temperature soundings every four hours in the Page vicinity. In addition, National Weather Service (NWS) surface and upper-air data were obtained for most of the Southwest for the period of the program. Two extra radiosonde measurements per day (total of four per day) were made at each of five NWS stations in the Southwest during the periods of the summer regional flights. Source measurements of aerosol size distribution and chemistry were made on several days. Emission rates, sulfur content, and other source operational parameters of the NGS were made available by SRP for the duration of the program. A summary of the VISTTA data base as it relates to model evaluation is presented in Section 4 of this report and by Seigneur et al. (1980).

3.2.2 Measurement Systems

During the summer, two aircraft were operated. The MRI Queen Air was used for both plume and regional measurements. The EPA-Las Vegas B-26 made only plume background and regional flights. In the winter, only the Queen Air was used. Table 1 lists the measurements made by the Queen Air and the B-26. The Queen Air system is described in more detail by Richards et al. (1981b) and the B-26 by Hering et al. (1981).

In the summer, the measurements listed in Table 2 were made at Zilnez Mesa aboard the UM mobile laboratory (see Sheppard et al., 1980). In both summer and winter, measurements were made at an SRP monitoring site in Page (the Boat Club) and at Copper Mine. An EPA van was used at Copper Mine to house many of the instruments in both summer and winter (Table 2). During the winter study, an HMC mobile laboratory was also sited at Copper Mine. The measurements made at Page are summarized in Table 3.

TABLE 1. MEASUREMENTS MADE ON MRI QUEEN AIR AND EPA/LV B-26

MEASUREMENTS MADE ON MRI QUEEN AIR
(Same for Summer and Winter)

CONTINUOUS MEASUREMENTS

SO_2	Condensation nuclei	Temperature
NO	Aerosol charge acceptance	Dew Point
NO_x	Indicated air speed	Turbulence
O_3	Position	Broad band radiation
b_{sp} (aerosol light scattering at 3 wavelengths)	Altitude	Ultraviolet radiation

AEROSOL SIZE DISTRIBUTION MEASUREMENTS

0.01-0.56 μm	Aerosol Charger/Mobility Analysis
0.56-about 5 μm	Optical Particle Counter with Multichannel Analyzer
0.8-15 μm	Axial Scattering Spectrometer Probe
0.090-3.0 μm	Optical Particle Counter

FILTER AND IMPACTOR SAMPLES

Filter Material	Analytical Methods
Teflon (2.5 μm precut)	IC:$SO_4^=$, NO_3^-; Colorimetry:NH_4^+;Selected filters:XRF,NAA
Prefired Quartz (2.5 μm precut)	GRALE:C; Light absorption
Teflon (0.1 μm precut)	XRF
Teflon followed by Nylon	Teflon: Archived;Nylon:IC NO_3^-(for HNO_3)
Teflon followed by Oxalic Acid impregnated glass	Teflon:Archived;OA filter:Colorimetric NH_4^+(for NH_3)
Teflon followed by Nylon wool packed tube (summer only)	Conversion to nitrobenzene and analysis by electron capture GC
Lundgren Impactor 50% cutoff diameters of 4,2,1 and 0.5 μm. Impactor stages are greased Mylar. Final filter is 0.4 μm Nuclepore	PIXE;Selected filters:NAA

NOTES: IC = ion chromatography, NAA - neutron activation analysis, GRALE = gamma-ray analysis for light elements, XRF - x-ray fluorescence, and PIXE = proton induced x-ray emission.

MEASUREMENTS MADE ON EPA-LV B-26
(Summer Only)

CONTINUOUS MEASUREMENTS

SO_2	Condensation nuclei	Position
O_3	Temperature	Pressure (Altitude)
b_{scat}	Dew Point	

AEROSOL SIZE DISTRIBUTION MEASUREMENTS

0.01-0.56 μm	Aerosol Charger/Mobility Analysis
0.12-1.0 μm	Optical Particle Counter

FILTER AND IMPACTOR MEASUREMENTS

Filter Material	Analytical Methods
Vaseline Coated Stainless Steel Substrates on low pressure impactor (LPI) 50% cut points 0.05 to 4 μm	Flash Volatization:S
Apiezon L Coated Mylar Substrates on LPI	PIXE
Ghia Corp. Unbacked Teflon(Cyclone precut)	Elemental analysis & Gravimetric mass:XRF & NAA
Pallflex Tissue-quartz (Cyclone precut)	GRALE: C;Light absorption

TABLE 2. MEASUREMENTS MADE AT ZILNEZ MESA AND COPPER MINE SITE

MEASUREMENTS MADE AT ZILNEZ MESA
(Summer Only)

CONTINUOUS MEASUREMENTS

SO2	Dew Point	Wind speed
NO	Condensation nuclei	Wind direction
NO_2	b_{sp}	Broad band radiation
O_3	Temperature	Ultraviolet radiation

AEROSOL SIZE DISTRIBUTION MEASUREMENTS

0.01-0.56 μm	Electrical mobility
0.56-5.0 μm	Light scattering
Total 0.56-5.0 μm	Rate meter
5.0-50.0 μm	Light scattering
Total 5.0-50.0 μm	Rate meter

OTHER MEASUREMENTS

Filter/Substrate	Analysis Technique
Teflon (<2.5 μm)	XRF
Nuclepore (<1 μm)	Mass(weighing);light absorption by integrating plate method
Metal strip (Low Pressure Impactor)	Sulfur by FVFPD
Greased Mylar (LPI)	PIXE , SEM
8 μm & 0.4 μm greased nuclepore-stacked filter	PIXE
Teflon (< 0.1 μm)	XRF
Quartz (<2.5 μm)	Carbon by GRALE
Nuclepore (<2.5 μm)	I.C. for nitrate, sulfate
Teflon/Oxalic Acid Coated glass-tandem filters	for Ammonia
Teflon/Nylon tandem	Nitric Acid by I.C. Analysis
Bubbler for H_2O_2	Liquid chemical fluorescence

MEASUREMENTS MADE AT COPPER MINE SITE

CONTINUOUS MEASUREMENTS

b_{sp}	SO_2 (W)	Temperature (W)
$NO\text{-}NO_x$ (W)*	Wind speed (W)	Dew Point (W)
O_3 (W)	Wind Direction (W)	

AEROSOL SIZE DISTRIBUTION MEASUREMENTS

0.01-0.56 μm	Electric Mobility
0.5-5 μm	Light Scattering

OTHER MEASUREMENTS

Filter/Substrate	Analysis Technique
Teflon (<2.5μm)(S)	XRF & Beta Gage
Teflon (<0.1 μm) (S)	XRF
Teflon (<2μm) (S)	XRF
Quartz (<2.5μm) (S)	Carbon by GRALE
Metal Strip (Low Pressure Impactor)(W)	Sulfur by Flash Volitalization, FPD Detection
Greased Mylar (Low Pressure Impactor)(W)	PIXE
Quartz (<2.5μm) (W)	Carbon by GRALE
Uncoated Nuclepore(<2.0μm) (W)	PIXE,I.C. for nitrate, sulfate
Greased Nuclepore (<2.0μm) (W)	PIXE
Nuclepore (<1.0μm) (W)	Mass and light absorption
8μm + 0.4μm Greased Nuclepore	PIXE
Bubbler for H_2O_2	Liquid chemical fluorescence

*W = winter only. S = summer only.

TABLE 3. MEASUREMENTS MADE AT PAGE SITE

Nephelometer	NO_x	Dichotomous Sampler
Telephotometer	Pyranometer	Radiosondes
Photographic	Pyroheliometer	Pibals
Ozone	Hi-Vol Sampler	Subjective Visibility Observations
SO_2 (summer only)		Surface Weather Observations
Anderson Hi Vol (summer only)		

3.2.3 NGS Emissions

The source measurements performed during the program are described by Candelaria and Palomino (1982). SO_2, NO_x, particulate mass, and other gas measurements were made in accordance with EPA Reference Test Methods 1-7. Particle size distribution measurements were made by a combination of techniques for different size ranges. Elemental composition analyses by neutron activation and wavelength dispersive X-ray fluorescence were performed on size-segregated samples. Particle size and chemistry data were also obtained by the MRI Queen Air in orbits close to the plant.

At this time, the summer source data have been fully analyzed (Candelaria and Palomino, 1982), and a small amount of winter source data is available; complete analysis of the winter data is in progress. During the summer program, combustion and precipitator problems were encountered with units one and two. Unit three operated normally.

The average particle size distribution of the unit three emissions measured in July can be reasonably well characterized by two log normal distributions. Approximately 99.75% of the mass was contained in a mode having an aerodynamic volume median diameter of approximately 5.7 μm and a geometric standard deviation of approximately 2.5. The remaining 0.25 percent of the mass was contained in a mode having an aerodynamic volume median diameter of about 0.27 μm and a geometric standard deviation of approximately 1.5. The estimated Stokes (physical) diameters of the two modes are 3.5 μm and 0.13 μm, respectively. No size distributions are available for units one and two, but the mass emission ratios for these units in July were over twice as large as the rate for unit three.

The coarse mode described above is presumed to be due to mechanical processes and the solidification of molten flyash. The fine mode is believed to be due to condensation of volatile emissions (Flagan et al., 1980; Markowski et al., 1980). Modes with similar median diameters were also measured in the Queen Air at distances within 20 km of the source. The fine mode measured in the Queen Air, however, peaked at about 0.04 um diameter instead of 0.13 um in the source, which suggests the possibility of additional condensation downstream from the source measurements or inconsistencies in calibration between the stack and aircraft sampling systems.

The elemental composition measurements were in reasonable agreement with what would be expected from analysis of the coal samples. The backup filters behind the size-segregating sampler (which collect particles smaller than 0.5 um diameter) were enriched compared to the larger particles collected in the cyclones in volatile elements such as S, Se, As, Ti, and Fe, as would be expected if condensation processes form the fine particle mode.

The average emission rates for all tests and all units during the summer study for particles, SO_2, and NO_x are summarized below in Table 4 (from Candelaria and Palomino, 1982). It should be noted, however, that the particulate emission rates varied greatly from test to test and unit to unit. In addition, the ratios of particulate and NO_x mass to SO_2 mass varied by up to a factor of two during the program, while the SO_2 emission rate per 10^6 BTU typically varied less than 15%. Similar variations were observed in the near-source Queen Air data (Richards et al., 1981b).

TABLE 4. SUMMARY OF AVERAGE NGS EMISSION RATES JULY 1-JULY 10, 1979 (FROM CANDELARIA AND PALOMINO, 1982)

	Particles		SO_2		NO_x	
	Average	Standard Deviation	Average	Standard Deviation	Average	Standard Deviation
ppm[a]	-	-	377	18	219	24
Lb/hr	610	296	7274	306	3027	393
Lb/10^6BTU	0.079	0.039	0.938	0.037	0.388	0.046

[a] Actual stack conditions.

3.2.4 Plume Chemistry and Aerosol Physics

Most of the plume chemistry and aerosol data were obtained during plume flights by the Queen Air (Richards et al., 1981b). Some aerosol size distribution data were also obtained during periods of plume impact at Zilnez Mesa (Wilson and McMurry, 1981). All plume chemistry data were obtained during sampling periods of limited duration under clean dry conditions typical of the southwestern U.S. No data were taken during moist conditions. Additional studies and analyses are under way to determine the representativeness of the sampling conditions and to obtain data under other conditions.

3.2.4.1 Nitrogen Chemistry (See Richards et al., 1981b for Details)

All airborne data are consistent with the EPA PLUVUE model in which emitted NO reacts with background O_3 as rapidly as the gases are mixed to produce the NO, NO_2, and O_3 concentrations predicted by the photostationary-state equations. There was no evidence of photochemical processes that produced NO_2 or O_3 by other chemical pathways. These results are consistent with those of earlier studies in the Southwest and were expected because of the clean dry background (Ogren et al., 1976, 1977). The aircraft data also indicate that no more than 3% to 6% of the NO_x was emitted as NO_2.

Nitric acid concentrations were an order of magnitude or more greater than aerosol nitrate concentrations for all measurements, both summer and winter. Comparisons of nitrate/NO_x ratios at two or more distances for numerous flights showed no evidence of aerosol nitrate formation in the plume. Ratios of $N(HNO_3)/N(NO_x)$, however, were measured as high as 17% at far downwind distances (89 km), and the conversion rate of NO_2 to vapor phase HNO_3 was estimated to be about 5.5% per hour for the above case, during midmorning hours.

Without exception, higher nitric acid concentrations were obtained in the plume orbits than in the background orbits in both the June-July and December studies. This was not the case for the sulfate data, because the plume excess sulfate concentrations were much lower in comparison to the variations in the background concentrations than was the case for nitric acid.

The conversion of NO_2 to vapor phase HNO_3 removes light absorbing NO_2 from the plume. It is recommended that the conversion of NO_2 to HNO_3 be included in plume visibility models, especially for distances greater than 50 km from the source. This reaction is included in the EPA PLUVUE model (Johnson et al., 1980).

Ammonia concentrations were measured to see if they were high enough that particulate nitrates might be formed in the plume (by reaction with nitric acid to form ammonium nitrate), and to see if more sulfuric acid than ammonia might be present in the plume. The ambient ammonia concentrations were typically high enough to neutralize all the sulfuric acid present, yet low enough that the saturation product for ammonium nitrate was not reached.

The ammonia concentrations converted to 1 atm and 25°C were typically 2 to 7 ug/m^3 in the summer and 0.1 to 2 ug/m^3 in the winter. The largest plume excess sulfate concentration measured was 0.76 ug/m^3, which would consume no more than 0.27 ug/m^3 ammonia; typical excess sulfate concentrations were much smaller. The ammonia and nitric acid data show that the plume was close to being saturated with respect to ammonium nitrate formation in the winter, but not in the summer. Under the conditions of the June-July and December 1979 study periods, the reaction of nitric acid with ammonia to form particulate nitrates does not appear to be needed in plume visibility models.

3.2.4.2 Sulfur Chemistry (See Richards et al., 1981b for Details)

In general, it was observed that measurable sulfate was formed from conversion of SO_2 only in dilute plumes and only during daylight hours. The greatest observed conversion of SO_2 to sulfate was 1.6% (at 89 km downwind on July 13) in the summer and 1% (at 115 km downwind on December 13) in the winter. No conversion was observed in early morning flights (before 0700 MST). The highest sulfate conversion rate measured on the aircraft (midmorning on July 13) was 0.8% per hour. For one clear midday case in the winter (December 12), the conversion rate was 0.2% per hour.

The measured conversion rates and ratios of products to reactants are consistent with the hypothesis that the oxidation of SO_2 and NO_2 is due primarily to the hydroxyl radical. Inspection of the OH data suggests that the background summer solar noon hydroxyl concentration was typically in the neighborhood of 1.2×10^7 cm^{-3}. This is sufficient to oxidize SO_2 at a rate of about 3% per hour (Sheppard et al., 1980).

Most models of secondary aerosol formation in plumes assume that sulfuric acid is the nucleating species. During the summer VISTTA study, the ammonia concentration was high enough that ammonia would react rapidly with any sulfuric acid formed. Sulfuric acid molecules would have a lifetime well under one second. With the measured SO_2 to sulfate conversion rates and ammonia concentrations, the steady state sulfuric acid vapor pressure would be far below the saturation pressure, and sulfuric acid could not have been the nucleating species. Analysis of the aerosol showed that there was

typically more than one, and less than two, moles of ammonium per mole of sulfate.

3.2.4.3 Secondary Aerosol Formation

Aerosol size distribution measurements were made on all passes through the plume by the Queen Air. In addition, size distribution measurements were made during plume impact at Zilnez Mesa in the summer. Measurements made during the plume chemistry orbits were analyzed to determine the aerosol formation rates in the plume (Richards et al., 1981b). Most of the measurable new aerosol volume in the summer was found in particles smaller than about 0.1 μm diameter, which are small enough to be quite ineffective at scattering light. Some formation might have occurred in particles larger than 0.1 μm, but it was small compared to, and indistinguishable from, the background aerosol. In total, relatively small amounts of new aerosol were formed compared to the amount of background aerosol. Secondary aerosol formation was found to be of minor importance in modeling the visibility impact of the NGS plume at distances less than 100 km for the dry conditions existing during this study.

From both the aircraft data and the Zilnez Mesa data, no evidence of new aerosol formation was found at night or before the plume had become well mixed with background air (SO_2 concentrations less than about 100 ppb). The best evidence of aerosol formation was found on July 13. On that day, little new aerosol was seen closer than 59 km downwind (2.5 hours downwind, sampled about 0830 MST); but between 59 km and 89 km, about 0.15 $\mu m^3/cm^3$ of new aerosol formed in the plume in the 0.01 to 0.1 μm size range, compared to 0.11 $\mu m^3/cm^3$ in the background in the same size range. The plume at 89 km was about 4.5 hours downwind. Some aerosol might have been formed in the range above 0.1 μm, but the formation was small compared to the background accumulation mode and was masked by variations in the background. The background contained about 1.2 $\mu m^3/cm^3$ in the accumulation mode (between 0.1 and 1.0 μm diameter) at 89 km. Measurement of the sulfate concentration above background at 89 km indicated that about 0.45 $\mu m^3/cm^3$ of sulfate (as ammonium sulfate) had formed. Thus, it is possible that on the order of 0.3 $\mu m^3/cm^3$ of new aerosol could have formed in the accumulation mode.

The aerosol formation rates in the winter were much slower than in the summer. Again, the amount formed was less than the variability in the background aerosol. The shape of the size distribution of the excess aerosol in the plume appeared similar from one distance to the next, except near the source where the dilution of the primary aerosol was apparent. The data show that secondary sulfate condenses on existing particles and also forms new particles.

McMurry et al. (1981), have examined the change in aerosol volume as a function of size and time for the July 13 data. They concluded that virtually all of the growth could be accounted for by condensational processes (homogeneous formation mechanisms). This result is consistent with the sulfate formation data and is further evidence that the secondary sulfate in the NGS plume formed from reaction of SO_2 and OH.

3.2.5 Plume Optics

The optical properties of the plume were measured in situ by the Queen Air (Richards et al., 1981b) and remotely by telephotometer (Bergstrom et al., 1981). The primary factors affecting light extinction by the plume and plume coloration are the primary aerosol emissions and the NO_2 concentrations. The formation of secondary aerosol was found to have a negligible effect on plume optics at NGS at distances up to at least 100 km from the plant.

At NGS, both source measurements (Candelaria and Palomino, 1982) and plume measurements (Richards et al., 1981b) show that there was little primary aerosol in the efficient light scattering range between 0.1 and 1.0 μm diameter. The bulk of the emitted aerosol mass was in the diameter range greater than 1 μm, and had a mass median diameter of about 3.5 μm. In this size range, the aerosol scatters light with about equal effectiveness at all visible wavelengths. Thus, the aerosol can contribute to extinction of light through the plume, and the light scattered by the aerosol into the line of sight can lower the contrast of distant targets viewed through the plume. The aerosol is not likely to contribute to plume coloration. The light scattering by the aerosol can also make the plume highly visible in forward scatter (e.g., in the early morning).

Bergstrom et al. (1981) tabulated the ratios of plume and sky intensity at the four wavelengths measured by the telephotometer for 15 total observations made during sight path flights on July 13, December 7, and December 15. The measurements were made at distances ranging from 4 to 30 km downwind with a median distance of 18 km. All of the measurements were made during periods when the plume was quite visible. The high, low, and median values of these measurements (presented in detail in Section 4 of this report) are given in Table 5. From these measurements it is clear that the primary optical effect of the plume occurs at wavelengths of 550 nm or less.

Richards et al. (1981b) calculated optical depths for the NGS plume from several passes through it due to both light absorption by NO_2 (using NO_2 data) and to scattering by the aerosol (using nephelometer data). The optical depths were calculated for the blue, green, and red wavelengths of

TABLE 5. PLUME INTENSITY/SKY INTENSITY

	405 nm	450 nm	550 nm	630 nm
High	0.94	0.94	1.00	1.03
Median	0.87	0.89	0.93	0.98
Low	0.76	0.81	0.88	0.94

the multiwavelength nephelometer. The extinction due to NO_2 is always much greater in the blue than in the red. (Blue light is absorbed and the plume looks reddish). For the cases calculated (up to 32 km downwind), the extinction due to particles always dominated in the red, but only dominated in the blue at distances usually less than 10 km from the source. For NGS, it was found that NO_2 could dominate the extinction in the green when about 1/4 of the NO_x was converted to NO_2, usually at a distance on the order of 20 km.

We conclude that, for the NGS plume, the reddish-brown coloration of the plume is generally due to NO_2 but the reduction in luminence of distant targets seen through the plume can be due to either NO_2 or primary aerosol. At distances less than about 10 km, the primary aerosol usually dominates the extinction at all wavelengths. For distances of 10 to 100 km, NO_2 can dominate the extinction in the blue and green as well as cause the coloration. Secondary aerosol sulfate is insignificant in affecting plume optics up to 100 km downwind.

3.2.6 Background Aerosol Composition and Contributions to Regional Haze in VISTTA Study Area

Data on the chemical composition of the regional haze in the VISTTA study area (Figure 1) were obtained at Zilnez Mesa and in both aircraft as part of VISTTA. Data were obtained at several other locations within the region as part of an EPA long-term regional monitoring program. Details of the Zilnez Mesa sampling system and analysis techniques are presented in Macias et al. (1981a). The regional surface sampling is described by Cahill et al. (1981). The VISTTA sampling was of limited duration and not all causes of regional haze were documented. Additional analysis is under way to determine the representativeness of the conditions measured during VISTTA.

From their network of regional filter and impactor samples, Cahill et al. (1981) have identified three aerosol patterns resulting in reduced

visibility in the southwestern desert areas. At Canyonlands National Park and Zilnez Mesa, regional visibility reduction is associated with:

1. Sulfur-rich transport from distant sources (urban areas, smelters, etc.),

2. Soil-derived elements (windblown dust), and

3. Forest fires.

At Zilnez Mesa during the 1979 summer VISTTA study, visibility reductions due to regional transport from distant urban sources and to forest fires were documented (Macias et al., 1981a, b). Table 6 (summarized from Macias et al., 1981a) shows the measured fine (less than 2.5 μm dia) and coarse particle species contributions to mass concentrations for conditions of urban air intrusion (6/30), forest fire impact (7/5) and low aerosol loading (7/10). Table 6 also presents the species contribution to light scattering for the same three days (Macias et al. 1981a).

As evidenced by Table 6, Macias et al. (1981a) and Ouimette et al. (1980) have concluded that the particle extinction at Zilnez Mesa was dominated by carbonaceous material and sulfate aerosol. Intrusions of urban air are identified by relatively higher sulfate and carbon levels. Forest fire aerosol is high in carbon but lower in sulfate. Forest fires are also characterized by higher potassium levels. Comparisons of fine particle sulfate to elemental sulfur and ammonium measurements by Macias et al. (1981a, b) indicate that the sulfur is largely in the form of ammonium sulfate with the possibility of some ammonium bisulfate. They also conclude that on the average, 88% of the fine carbon was in organic compounds with the remainder being soot.

Ouimette et al. (1980) calculated the species contribution to the particle extinction coefficient at Zilnez Mesa. An average for twelve sets of samples (including a significant bias due to forest fire intrusion) showed that 39% of the extinction was due to nonsoot carbon compounds, 22% to ammonium sulfate, and 11% to absorption by soot carbon. The total average extinction coefficient due to particles (b_{sp}) during collection of the twelve samples was 17×10^{-6} m^{-1} (less than the equivalent of twice Rayleigh scatter). They concluded that the measured species could account for $94 \pm 19\%$ of the fine aerosol mass concentration and $85 \pm 34\%$ of the measured particle extinction coefficient. In addition they concluded that the submicron aerosol species contributed to the particle scattering coefficient in approximately the same proportion that they contributed to the fine particle mass concentration. Water was ignored in all of the above estimates since the relative humidity was usually less than 10%.

TABLE 6. CHEMICAL SPECIES MASS AND EXTINCTION BALANCE FOR ZILNEX MESA: JUNE 30, JULY 5, JULY 10, 1979 (FROM MACIAS ET AL., 1981a)

Compound	Fine Particle (< 2.5 μm) Mass Balance 6/30	7/5	7/10
$(NH_4)_2 SO_4$	46%	9.4%	30%
Organic Carbon	34%	53%	24%
K_2O	3.3%	5.6%	2.8%
Fe_2O_3, Al_2O_3, NH_4NO_3, CuO, ZnO, PbO, soot	6.3%	5.3%	23%
Undetermined	~10%	~27%	~20%
Total fine mass	8.4 $\mu g/m^3$	14.7 $\mu g/m^3$	3.0 $\mu g/m^3$

Compound	Coarse Particle (2.5 - 15 μm) Mass Balance 6/30	7/5	7/10
SiO_2	30%	28%	40%
Al_2O_3, Fe_2O_3	10.2%	12.4%	15.9%
$CaO, K_2O, (NH_4)_2SO_4$			
CuO, ZnO, PbO	9.9%	13.5%	13.5%
Undetermined	~50%	~46%	~31%
Total coarse mass	13.8 $\mu g/m^3$	10.2 $\mu g/m^3$	6.3 $\mu g/m^3$

	Calculated Particle Light Extinction - Species Contribution 6/30		7/5		7/10	
	$b(10^{-6}m^{-1})$	$\%b_{ep}$	$b(10^{-6}m^{-1})$	$\%b_{ep}$	$b(10^{-6}m^{-1})$	$\%b_{ep}$
Fine particles (<2.5 μm)[a]						
$(NH_4)_2SO_4$	9.9	33[b]	6.8	11	1.1	11
Organic carbon	9.0	30	30	48	2.1	20
Elemental carbon	3.6	12	9.6	15	1.1	11
$(b_{ap} + b_{sp})$[b]	(3.0+0.6)		(8.2+1.4)		(0.8+0.3)	
Other fine	3.1	10	12.8	20	3.6	34
Coarse particles[c]	4.5	15	3.7	6	2.5	24
Total b_{ep}	30.1	100	62.9	100	10.4	100

[a]Scattering due to specific species were obtained from Ouimette (1980) Table 3.12 multiplied by the ratio of the masses given in Table 5 of Macias et al., 1981a, to Ouimette Table 3.5 unless otherwise stated.

[b]b_{ep} = Light extinction due to particles ($b_{ep} = b_{sp} + b_{ap}$). b_{sp} = Scattering due to particles. b_{ap} = Absorption due to particles.

[c]Coarse particle contribution was calculated from number size distribution (McMurry et al., 1980) and Mie coefficients then scaled to the ADS/Tef coarse mass in Table 5 of Macias et al., 1981a (scaling factor was 1.1 for all days).

Ouimette (1980) has calculated the average species contribution to aerosol mass as a function of particle size for twelve Zilnez Mesa samples. The minimum in the average size distribution is at about 1 μm diameter with a substantial change in the elemental composition above 1 μm. Both sulfur and carbon decrease and silicon dioxide increases dramatically above 1 μm. For sampling in the Southwest, it is apparent that for a dichotomous sampler, the cut point should be about 1 μm to minimize distortion of the fine particle sample by coarse particles (windblown dust).

3.2.7 Regional Haze - Transport and Distribution

The transport and distribution of the southwestern haze were examined for several days during the summer 1979 sampling period by Macias *et al.* (1981b) and by Hering *et al.* (1981). Surface chemistry data from Zilnez Mesa and other southwestern sources, aircraft data from regional flights, and upper air and surface meteorological data were examined to determine the source and spatial extent of the southwestern haze for several days. Nephelometer data from Bryce Canyon and Zilnez Mesa were examined by Babson *et al.* (1982) for the three weeks of the summer program to determine the degree of correlation (homogeneity) between the two sites, which are about 160 km apart.

3.2.7.1 Transport from Southern California: June 29-30, 1979

June 29 was one of the hazier periods observed during the program with a 24-hour average b_{sp} measured by the nephelometer at the Zilnez Mesa site of 24×10^{-6} m^{-1}. Aircraft flights from Farmington, New Mexico, to Las Vegas, Nevada, on the afternoon of the 29th indicated that the haze was widespread and quite uniform extending up to 3000 m MSL, with an average b_{sp} of 26×10^{-6} m^{-1} (Hering *et al.*, 1981). Trajectory analyses constructed independently from both surface and upper-air wind measurements indicated that the air at Zilnez Mesa had originated in the southern California coastal area one to two days earlier. From June 25 to June 28, the southern California region experienced a strong stagnation condition during which sulfate and oxidant levels built up. The pollutants, accumulated over several days, were transported east on the 29th and 30th.

On the 30th, the sulfur size distribution at Zilnez Mesa had a median diameter of 0.30 μm (Macias *et al.*, 1981b). The typical mass median diameter at Zilnez Mesa on other days was about 0.2 μm, which is typical for the desert Southwest (Ouimette, 1980). The distributions measured in the coastal Los Angeles basin typically have a median diameter greater than 0.5 μm (Friedlander, 1980). The relatively large sulfur size on the 30th provides an additional indication that the Zilnez Mesa data were influenced by southern California emissions. The lead concentration also increased substantially on the 30th, again indicating a potential urban source.

3.2.7.2 Forest Fire Plumes: July 4-5, 1979

This period had the highest average particle scattering coefficient observed during the program at Zilnez Mesa. The 24-hour average for the 5th was 51×10^{-6} m^{-1} with a peak hourly average of 141×10^{-6} m^{-1}. Trajectory data as well as visual observations indicated the primary source of the haze was a series of forest fires about 100 to 150 km away (Macias et al., 1981b). The fine aerosol samples at Zilnez Mesa were characterized by carbon concentrations over twice that of June 30 but sulfate concentrations less than half of the 30th (Table 6). The fires were indicated in nephelometer measurements made throughout the region, including Grand Canyon, Copper Mine, and Bryce Canyon.

3.2.7.3 Other Days

Days of very low scattering coefficient, such as July 10 with b_{sp} of 6×10^{-6} m^{-1}, were measured several times during the winter and occasionally during the summer. Even on these days, sulfates and carbon compounds accounted for much of the aerosol, and elements like lead and copper were present, indicating a significant anthropogenic contribution to the aerosol that was there.

During the study, there was no obvious evidence of the copper smelters in southern Arizona. However, the sampling periods occurred during times when the prevailing flow was more westerly than southerly. Additional sampling later in the summer might show the effects of the moist southerly flow which could bring the smelter emissions into the Page area.

3.2.7.4 Bryce Canyon-Zilnez Mesa Comparison

Babson et al. (1982) compared nephelometer measurements made simultaneously at Bryce Canyon and Zilnez Mesa. For the three weeks of the summer program, the correlation coefficients between the hourly averages at the two sites were: June 27-30, 0.772; July 1-7, 0.044; July 8-13, 0.263.

The first period was characterized by an intrusion of regional haze from the southern California area, and the correlation coefficient indicates a reasonably homogeneous atmosphere. The second week was affected by forest fires, which are likely to affect a smaller area at any given time; hence correlations are low. The third week was, in general, cleaner and free from major episodes. These correlations indicate that the atmosphere of the desert Southwest is often inhomogeneous over distances of 150 km (July 1-13). Comparison of the average scattering coefficients (b_{scat}) at the two sites for the third week, however, indicate that the inhomogeneities can average out with time. For Bryce Canyon during July 8-13, b_{scat} averaged

20×10^{-6} m^{-1} compared to 17×10^{-6} m^{-1} at Zilnez Mesa. When they occur, episodes of regional haze can be quite homogeneous over hundreds of kilometers (June 27-30).

3.3 MODEL EVALUATION

One of the goals of the VISTTA project is to acquire data for evaluation of visibility models. Bergstrom et al. (1981) have described a preliminary evaluation of EPA's PLUVUE visibility model, using cases described in Section 4 of this report. Only a cursory discussion of the model and evaluation techniques is presented in this report.

The EPA plume visibility model, PLUVUE, developed by Systems Applications, Inc. has been evaluated by Bergstrom et al. (1981) using the VISTTA data obtained at NGS. The complete model starts with the emissions and meteorological conditions as input and computes the optical properties of the resulting plume. PLUVUE accounts for transport and dispersion, gas-to-gas and gas-to-particle reactions, particle growth, surface deposition, and the optical and chemical properties of the background. The individual model components were evaluated separately for 15 different Queen Air passes through the plume along telephotometer sight paths between 4 and 40 km downwind of the plant. The passes were generally perpendicular to the plume axis. The data most useful for plume visibility model evaluation have been selected from these results and are presented in Section 4.

3.3.1 Dispersion Module

The dispersion module of PLUVUE is based on a Gaussian formulation. Instantaneous plume widths and concentrations and the resulting dispersion coefficients were compared to Pasquill-Gifford-Turner dispersion averages. When fairly constant wind directions and atmospheric stability were observed, the dispersion coefficients and centerline concentrations could be predicted within about a factor of two. However, with a varying wind field (meandering plume and wind shears) the horizontal dispersion coefficients were sometimes dramatically underpredicted while the centerline concentration was still within a factor of two, indicating a non-Gaussian plume shape. For the evaluation of the other model components, the horizontal dispersion coefficients were adjusted to agree with the aircraft measurements of plume width.

3.3.2 Chemistry and Aerosol Module

The chemical module involves nine reactions among NO, NO_2, O_3, O_2, SO_2, OH, H_2O, and O('D). For the VISTTA cases, the background

hydrocarbon concentrations were assumed to be very small, based on the observations of Sheppard et al. (1980). Even so, it was found that the calculated chemical rates were sensitive to the assumed hydrocarbon concentrations. The model assumes that NO is oxidized to NO_2 by O_2 in small amounts (termolecular oxidation) and by O_3. NO_2 and SO_2 are oxidized by OH. The model generally overestimated the plume centerline NO_2 concentrations but underpredicted NO_2 concentrations closer to the plume edge. This was assumed to be due to an overprediction of the rate of diffusion of ozone into the plume. For the distances evaluated (less than 40 km), the rate of oxidation was predicted to be less than 0.02% per hour for NO_2 and negligible for SO_2. This is in agreement with the Queen Air measurements at these distances for which secondary aerosol formation was undetectable (Richards et al., 1981b). Both the model and the measurements indicate that secondary aerosol formation is not important for visibility impairment at NGS for the distances and conditions studied.

3.3.3 Optics Module

The optics module calculates the radiative properties of the plume and their optical effects. This component of the model was evaluated using observed aerosol and NO_2 concentrations along the sight path to compute the ratio of plume intensity to sky intensity and the plume contrast at 405 nm, 450 nm, 550 nm, and 630 nm (the wavelengths of the telephotometers used). For twelve cases on December 7, the calculated results generally agreed with the telephotometer measurements, with the model overpredicting the optical effect of the plume.

3.3.4 Overall Model Evaluation

The complete model was evaluated for 15 cases using emissions, meteorological and chemistry data presented in Section 4. Plume pollutant concentrations and plume/sky intensity ratios were calculated as model outputs. The only input parameters adjusted were horizontal and vertical dispersion coefficients, which were determined from aircraft measurements.

The average relative errors between the measurements and model predictions for the NO_x and SO_2 concentrations were 16.3% and 25.3%. The average relative error for the light scattering coefficient was about 50%. This error is due in part to the large uncertainties in the large particle emissions and to the fact that some large particles are lost in the inlet system of the aircraft nephelometer. The plant aerosol emissions were highly variable, and measurements were made on only one of three stacks at any one time. The model tends to overestimate the plume impact. The greatest uncertainties are in the diffusion module, which has the limitations associated with all Gaussian diffusion models.

A sensitivity analysis was carried out for one set of input conditions. Simulations were run for various scenarios of reduced input concentrations (emissions) of NO_x and particles. The calculated visibility impairment for these runs was found to be due primarily to plume discoloration due mainly to light absorption by NO_x.

3.4 METHODS COMPARISONS

The VISTTA project has provided the opportunity for a variety of instrument and methods intercomparisons. The telephotometers used during the program were all intercompared and calibrated against standard light sources (Bergstrom et al., 1982); telephotometer measurements were compared with nephelometer measurements throughout the region and along sight paths (Babson et al., 1982; Bergstrom et al., 1982; Richards et al., 1981c) and various methods of measuring aerosol sulfur were compared (Macias et al., 1981a).

3.4.1 Telephotometers Comparisons

Bergstrom et al. (1982) found in comparing 12 MRI Model 3010 telephotometers under laboratory conditions that the average inherent error in the sky/target intensity ratio was about 1% but that the errors in the absolute radiance averaged about 10%. Although the manufacturer of a lamp used as a calibration source specified the uncertainty in the lamp at 2%, comparison of two lamps indicated a difference of 10% in lamp intensity. Analysis of extensive simultaneous field measurements by sets of two telephotometers showed that when operator variations are included in the comparison, the error in the sky/target intensity ratio increases to about 2%, with an average difference of 15% between operators in the calculated extinction coefficient (Bergstrom et al., 1982). Variation was less using only high contrast cases.

3.4.2 Telephotometers-Nephelometer Comparisons

Two different types of telephotometers, a surface-based Integrating Nephelometer, and an airborne nephelometer, all making regional (not plume) measurements, were intercompared (Bergstrom et al, 1982). The average extinction coefficient (for green light) along paths to four targets observed from Zilnez Mesa was 25×10^{-6} m^{-1} for the University of Vienna telephotometer (Horvath, 1981) and 29×10^{-6} m^{-1} for the MRI telephotometer. At the same time, a modified MRI 1560 Integrating Nephelometer at Zilnez Mesa recorded an aerosol scattering coefficient (b_{sp}) of 22×10^{-6} m^{-1}. A multiwavelength nephelometer on a sight path flight from Zilnez Mesa to Navajo Mountain (35 km northwest) also recorded an

average b_{sp} along the flight path of 22×10^{-6} m^{-1} for green light. The difference between the nephelometer and telephotometer results is due largely to the contribution of absorption to the telephotometer-measured extinction coefficient and the partial efficiency of the nephelometer in the measurement of light scattering by large particles. Additional comparisons between telephotometer and nephelometer data have been made by Richards et al. (1981c), and preliminary results published.

Babson et al. (1982) compared nephelometer scattering coefficient measurements with calculations of extinction coefficient from telephotometer measurements for twelve different targets made simultaneously at Bryce Canyon from June 27 to July 13 1979. The correlation coefficients ranged from 0.93 to 0.52 for the different targets. The best correlations were obtained for targets to the north between 60 and 100 km distance. The worst correlations were for targets to the WNW, ESE, and SW, all of which were subject to changes in inherent contrast as the sun moves across the sky. Correlating the nephelometer readings with the average of the readings for the three northerly targets between 60 and 100 km distant for the three-week period gave a correlation coefficient of 0.95. Plots of correlation coefficients for 10 targets as a function of time of day showed the best correlations to occur at noon for all targets. All noon correlations were above 0.87.

3.4.3 Sulfur Measurements

A total of seven different size-segregating samplers were used at Zilnez Mesa for the collection of sulfur aerosol. The sample substrates were analyzed by one of four techniques: Ion Chromatography (I.C.), X-Ray Fluorescence (XRF), Proton Induced X-Ray Emission (PIXE), or Flash Volatilization/Flame Photometric Detection (FVFPD). The sulfur values were intercompared for at least eleven different runs. The correlation coefficient (r) was greater than 0.92 for all comparisons of all seven techniques (Macias et al., 1980). Some systematic differences did occur but these are believed to be due at least in part to differences in cut point of the size-segregating devices. The average standard deviation of the methods was 24%. The good correlation between the methods provided information on the chemical form of the fine particle sulfur. I.C. sulfate analysis and PIXE sulfur analysis of the nuclepore filter following the AlHL cyclone separator had a correlation coefficient of greater than 0.99. The slope, 3.07, indicated that the sulfur was essentially all in the form of water soluble sulfate.

3.5 DISCUSSION

One of the general objectives of the VISTTA experiments is to put in perspective the contribution of power plants to the southwestern regional

haze. To this end, it is useful to compare the reduction in visual range due to the plume alone to the reduction due to the regional haze transported to the Page area from Southern California. Since the VISTTA study was of limited duration, we have not determined the representativeness of the regional transport condition. We present this comparison only as a means of demonstrating the relative effects of the plume and not as a means of demonstrating the typical cause of visibility impairment at Page.

Richards et al. (1981b, Table 12) have tabulated the optical depths due to NO_2 and light scattering aerosol for several aircraft passes through the NGS plume at distances less than about 30 km. These passes are the same ones used by Bergstrom et al. (1981) in their evaluation of PLUVUE. The passes were perpendicular to the plume and represent well-defined (worst-case) plumes. In the green (550 nm), the average optical depth due to NO_2 and light scattering aerosol for the eleven cases calculated was 0.4.

Assume that the plume is emitted into a clean (Rayleigh Scattering) atmosphere with a scattering coefficient of 12×10^{-6} m^{-1}, and that the visual range is given by the Koshmieder relationship:

$$\text{Visual Range} = \frac{3.91}{\text{Extinction coefficient}};$$

where 3.91 is the optical depth of the atmosphere between the observer and a target at the limit of visibility (0.02 contrast). The visual range VR (for green light) looking through the plume would be given by:

$$VR = [3.91 - (\text{Plume optical depth})]/(\text{Rayleigh scattering coefficient})$$

$$= \frac{3.91 - 0.4}{12 \times 10^{-6}} \text{ m} = 292 \text{ km}.$$

For comparison, the extinction coefficient due to particles on June 30 1979 at Zilnez Mesa, during conditions of regional transport from Southern California was 30×10^{-6} m^{-1} (Table 6). The visual range due to the regional aerosol was thus:

$$VR = 3.91/(\text{Aerosol extinction coefficient} + \text{Rayleigh scattering coefficient})$$

$$= \frac{3.91}{(30 + 12) \times 10^{-6}} \text{ m} = 93 \text{ km}.$$

The NGS plume at the distances measured was typically under 10 km wide. The regional haze on the other hand was several hundred km across.

Another way of stating the results from this comparison is that a 22 km path length through the regional haze would have an optical thickness 0.4 greater than the optical thickness for the same path length with only Rayleigh scattering by air. Thus, in this example, when the plume is dispersed to a width of 22 km, the average contribution of the plume to light extinction within its width is the same as the local contribution of the regional haze.

From the above comparison, we can see that in the southwestern U.S., haze transported from regional sources far away can have an effect on visibility and therefore on the visual air quality in scenic areas that is equal to or greater than the effects due to a nearby well-controlled power plant.

SECTION 4

CASE STUDIES FOR PLUME VISIBILITY MODEL EVALUATION

Prepared by:

C. Seigneur, A. B. Hudischewskyj, B. L. Babson, and R. W. Bergstrom
Systems Applications, Inc.

S. L. Eigsti*
Meteorology Research, Inc.

4.1 CASE STUDY INTRODUCTION

One of the issues to be addressed by the EPA toward the purposes set forth by the 1977 Amendments to the Clean Air Act is the evaluation of the effect of plumes emitted from large point sources, such as power plants or smelters, on atmospheric visibility in mandatory class I areas. Accordingly, plume visibility models have been developed to simulate the visual effects of plumes. Because the performance of a mathematical model must be carefully evaluated before it can be used in a predictive manner, a goal of the VISTTA field programs conducted in June-July and December 1979 was to provide a data base for the evaluation of plume visibility models. The VISTTA data are available from Sonoma Technology Inc. (STI), Santa Rosa, California.

A summary of the data presented in this section and of the activities of the field programs is presented in Table 7. Measurements of the emission rates and the characteristics of the power plant were carried out and meteorological data were obtained along with background trace gas and aerosol concentrations at various sites. The visual effects of the plume were measured by means of telephotometers. Plume concentration measurements were performed with an instrumented aircraft (MRI Queen Air); the aircraft made continuous measurements of SO_2, NO_x, and O_3 concentrations and aerosol scattering coefficients. The flight paths were aligned with the telephotomer sight paths so that concentration measurements throughout the plume were made at the plume downwind distance that corresponded to the telephotometer measurements.

---

*Current Affiliation: Qume Corp., San Jose, California

TABLE 7. PROGRAM ACTIVITIES

(a) Program I--June-July 1979

Date (1979)	Activity	Referenced Table*	Comments†
June 27	Plume chemistry		
June 28	Plume visibility	13	Stable plume early
June 29	Regional haze		
July 1	Plume visibility		Plume dispersed; hazy
July 2	Plume chemistry		Plume dispersed; hazy; low concentrations
July 3	Regional haze		Fires and smoke in the south
July 5	Plume visibility		Very hazy as a result of forest fire smoke
July 6	Plume chemistry		Smoke near the Grand Canyon
July 7	Regional haze		
July 9	Plume chemistry		
July 10	Plume visibility		Hazy background
July 11	Regional haze		
July 13	Plume chemistry	13	Good plume chemistry and telephotometer data

(b) Program II--December 1979

Date (1979)	Activity	Referenced Table*	Comments‡
December 3	Plume chemistry		Plume both east and west
December 4	Plume visibility	13	Cloudy sky
December 5	Plume chemistry		Orbits at 30 and 80 km downwind
December 7	Plume visibility	13	Good telephotometer data, morning and afternoon
December 9	Plume chemistry		Orbits at 30, 60, and 90 km downwind
December 10	Plume visibility		Hazy, light plume
December 12	Plume chemistry		Measurements to 100 km south late in day
December 15	Plume visibility	13	Darkest plume measured

* This table is presented in Section 4.3 of this report.
† Richards (1980).
‡ Richards (1981a).

A more detailed description of the VISTTA data base is presented in Seigneur et al. (1980), and the results of the model simulations using the EPA/SAI plume visibility model have been described by Bergstrom et al. (1981). This section presents case studies from the data base itself, which can be directly used for the evaluation of plume visibility models. Such visibility models consist of relatively independent components (e.g., an emission module, a transport and diffusion module, and a chemistry and aerosol dynamics module), which are linked together to relate specific emission and meteorological conditions to the observed visual effect of a plume; to adequately assess a complete model, each component must be evaluated individually. In this way, the overall sensitivity and uncertainty of the model can be ascertained. Therefore, this section presents the data base that is suitable for the overall evaluation of a plume visibility model, as well as data that are useful for the evaluation of the individual components of a plume visibility model.

Section 4.2 describes the data base for the overall evaluation of plume visibility models, along with plume measurements (i.e., plume width and plume concentrations) that can be used for evaluating the dispersion and chemistry components of a plume model. Section 4.3 describes the data base for the evaluation of the optics component of a visibility model. In each of these sections, the uncertainty associated with the measurements and the sensitivity of model performance to input data are discussed.

The data bases used in these case studies are tabulated in Section 4.3. Detailed data from VISTTA are available from MRI or STI as follows:

> Aircraft data

- Richards, L. W. (1980)
- Richards, L. W. (1981a)

> Telephotometer data

- Systems Applications, Inc. (1981a)
- Systems Applications, Inc. (1981b)
- Hogo, H., et al. (1981)

> Ground photographic data

- Hudischewskyj, A. B., et al. (1981)

4.2 DESCRIPTION OF THE DATA BASE FOR PLUME VISIBILITY MODEL EVALUATION

A data base for plume visibility model evaluation must comprise various sets of model input data, as well as measurements that can be

compared with model predictions:

- Data on the relative location of the sun, plume, and observer.
- Emission data (flue gas characteristics and emission rates).
- Meteorological data (wind speed, wind direction, temperature, and relative humidity).
- Background trace gas, aerosol, and visual range data.

Measurements of the plume characteristics are also needed to evaluate the performance of the plume visibility model. For this study, plume contrasts were measured by means of four-wavelength telephotometers. The plume width and plume concentration data (trace gas and particulates), which were measured by the aircraft, could also be used to independently evaluate different components of a plume visibility model such as the diffusion module or the chemistry module.

A large amount of data was collected for plume visibility modeling during the 1979 VISTTA field programs. To evaluate a mathematical model, however, it is necessary to use experimental data that offer consistency and reliability. Steady meteorological conditions and a fairly cloud-free sky are needed to obtain a coherent set of data for model evaluation relating to visibility impairment by a plume in the atmosphere. During the 1979 VISTTA programs, three days provided measurements of a well-defined plume against a clear sky: July 13, December 7, and December 15, 1979. The best day for obtaining plume data during the summer program was July 13; although the activities on that day were not designed for visibility evaluation, a flight path of the aircraft corresponded to two telephotometer plume targets. On December 7 1979 the plume was fairly stable and, consequently, a large amount of data was obtained during the morning and afternoon. On December 15 1979 the darkest plume was observed.

To evaluate the performance of the plume visibility model using a gray background, two additional days were considered. On June 28 1979 telephotometer measurements of a stable plume were made with the Navajo Mountain (dark gray) in the background. On December 4 1979 a fairly homogeneous cloud layer, which could be approximated with a light gray background in a plume visibility model, was observed behind a stable plume.

The complete data base for plume visibility model evaluation involves 28 cases using these five days and is presented in Section 4.3. In this

section, we discuss the development of the data base and the uncertainties associated with the input data. Figures 3 through 8 present maps of the area for each set of case studies showing the telephotometer sight paths, the aircraft flight path, and the plume trajectories. When the aircraft path and telephotometer sight path coincide, only the sight path and the two plume centerlines that correspond to the minimum and maximum value of the wind direction angle are shown. The instruments used for the measurements and associated uncertainties are listed in Table 8.

4.2.1 Plume-Sun-Observer Geometry

The source and observer locations are given by UTM coordinates and by elevation with respect to mean sea level. The plume-observer geometry is computed by a plume visibility model from these source and observer locations and from plume geometry. The sun position (zenith and azimuth angles) is computed by a visibility model from the time of the measurement. Because telephotometer measurements typically take about five to ten minutes, the time uncertainty can be considered to be on the order of five minutes. The scattering angle is then computed from the sun position and the plume-observer geometry. Uncertainties in the scattering angle are likely to arise from uncertainties in the plume location, rather than from the observer location or the sun position. Calculation of the plume location is discussed in Section 4.2.3.

4.2.2 Emission Data

A plume visibility model requires data on flue gas characteristics to calculate plume rise and the NO_2/NO_x ratio in the emissions, as well as data on the emission rates of primary pollutants (i.e., NO_x, SO_2, and primary particulates).

4.2.2.1 Flue Gas Characteristics

Flue gas characteristics (i.e., oxygen content, temperature, flow rate, and exit velocity) were obtained from the Salt River Project/Navajo Generating Station (SRP/NGS). Uncertainties in plume rise calculations did not affect visibility calculations noticeably for the plume-observer geometry data considered.

The oxygen content of the flue gases affects the conversion of NO to NO_2 in the hot flue gases when the termolecular reaction $2NO + O_2 \rightarrow 2NO_2$ takes place. The oxygen mole content did not vary by more than 1% during the sampling periods used for the two VISTTA programs, and the plume

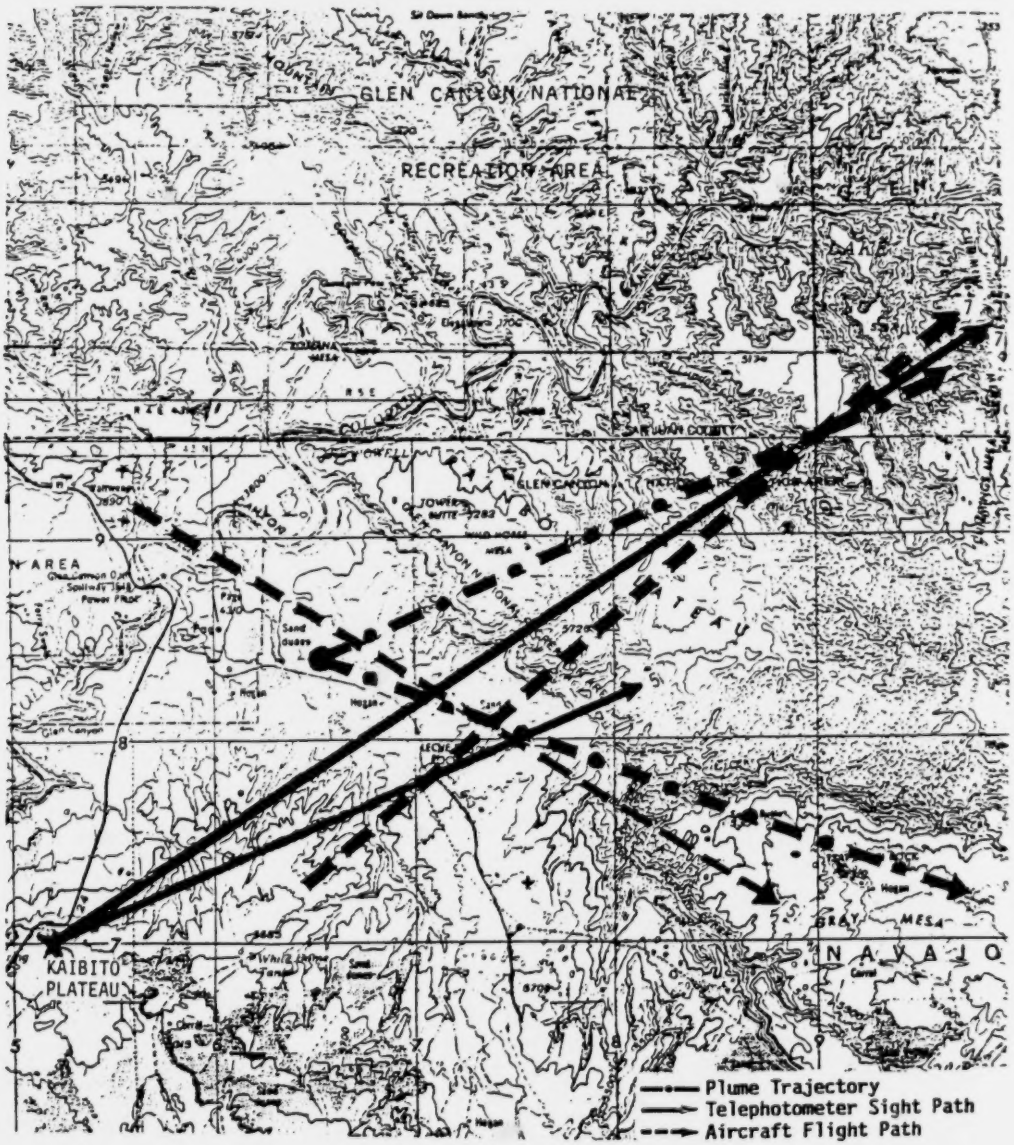

Figure 3. Case studies: June 28, 1979.

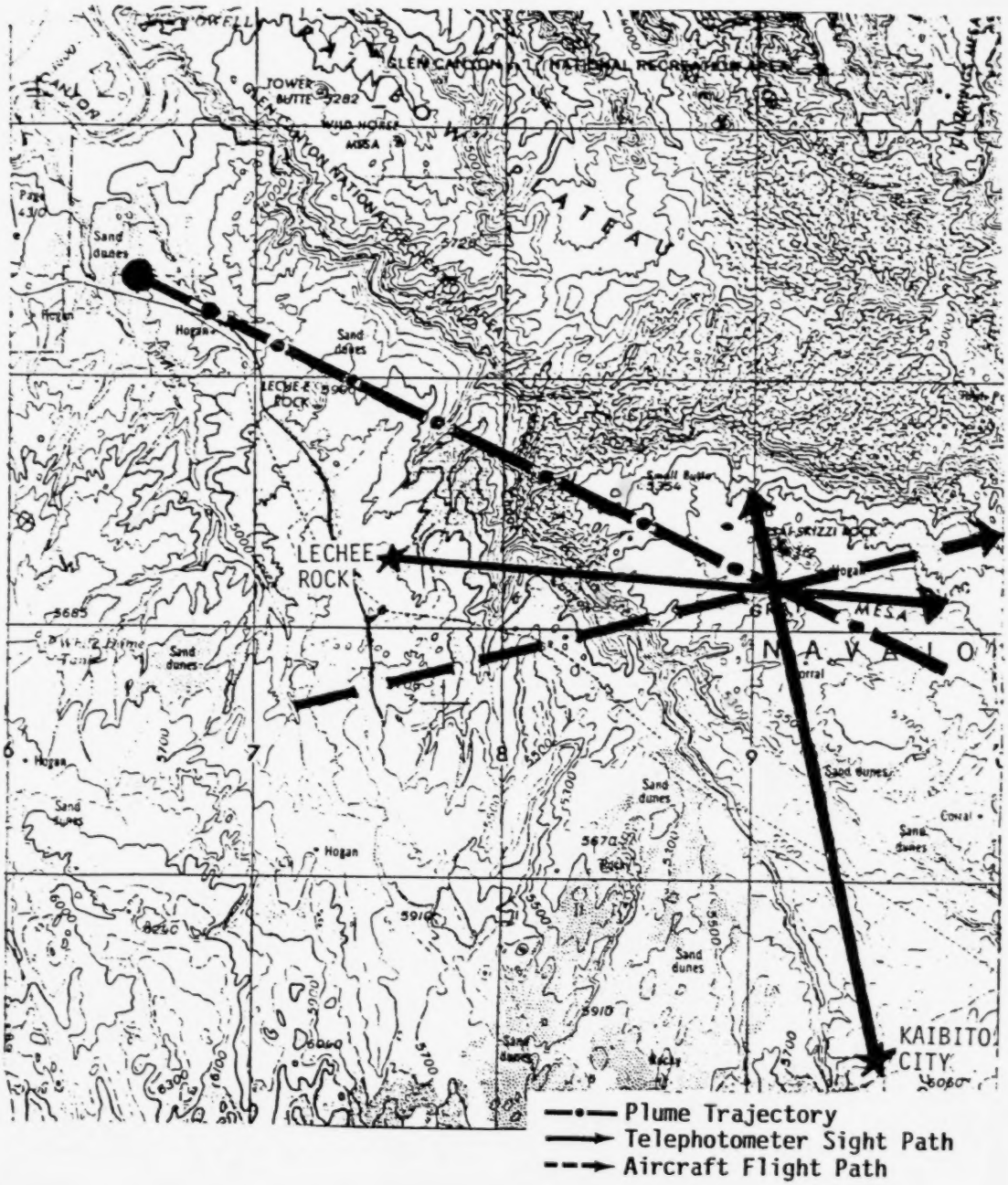

Figure 4. Case studies: July 13, 1979.

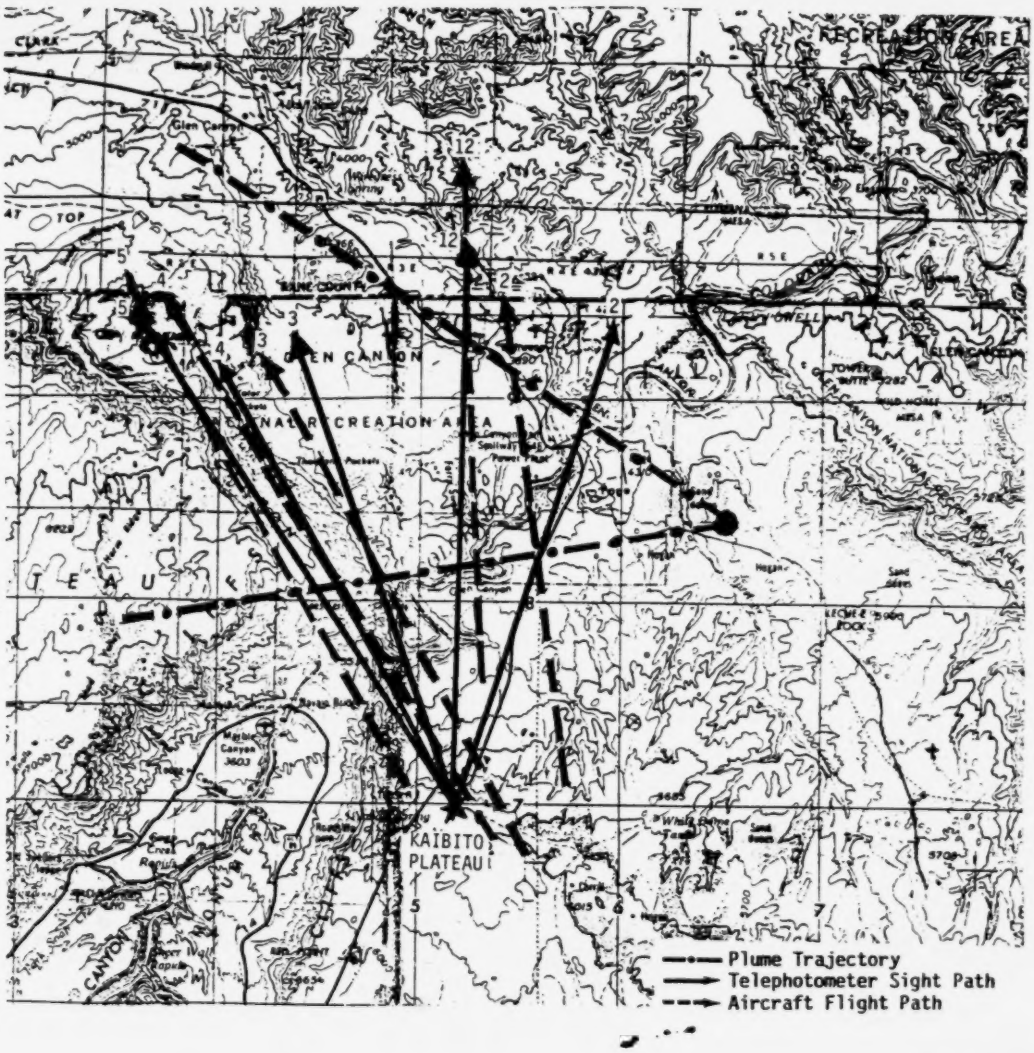

Figure 5. Case studies: December 4, 1979.

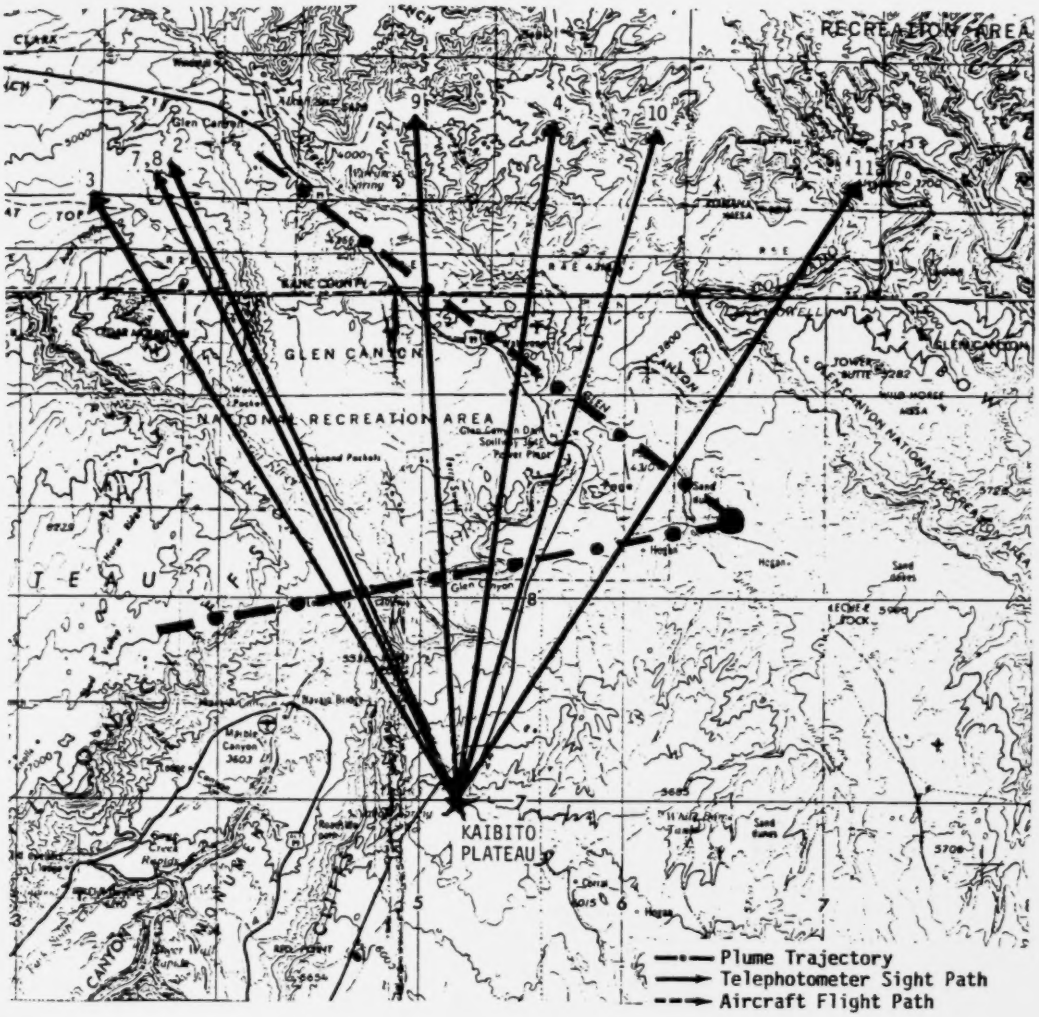

Figure 6. Case studies: Morning of December 7, 1979.

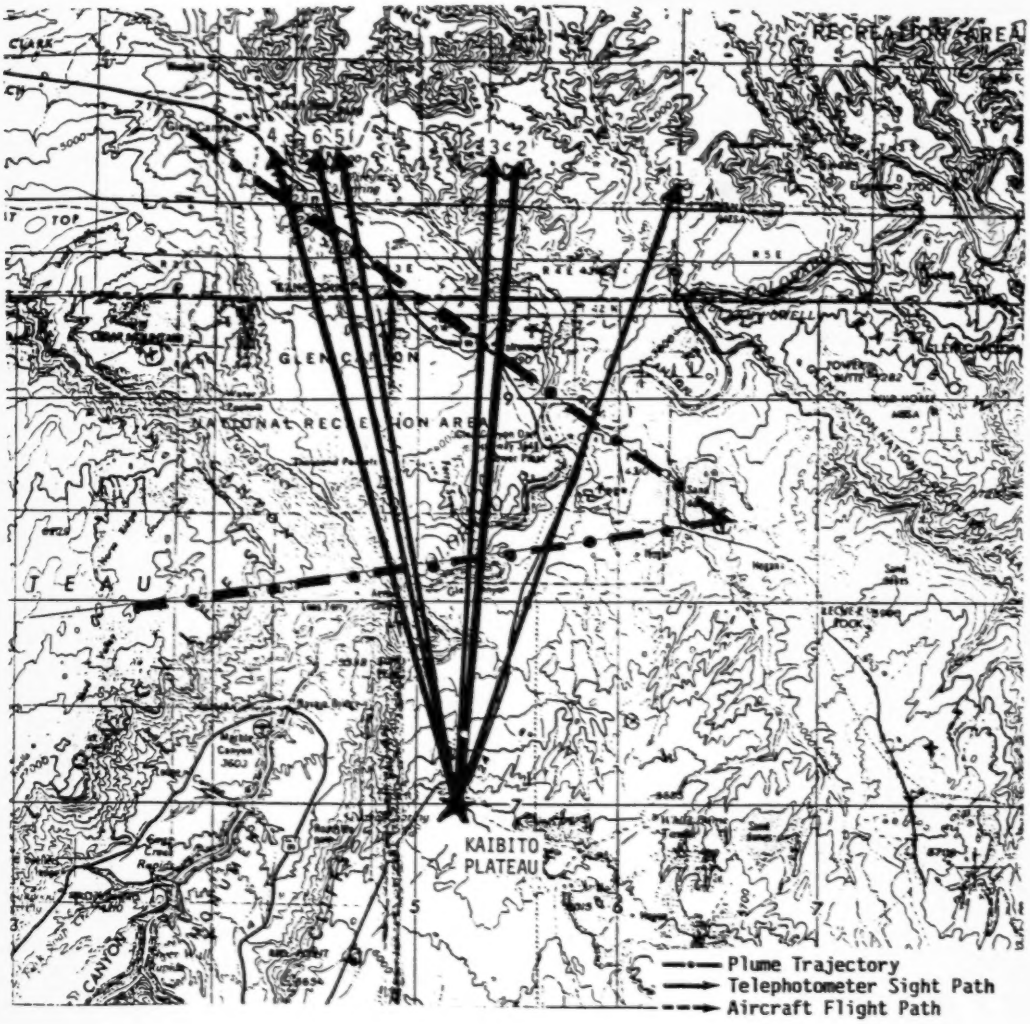

Figure 7. Case studies: Afternoon of December 7, 1979.

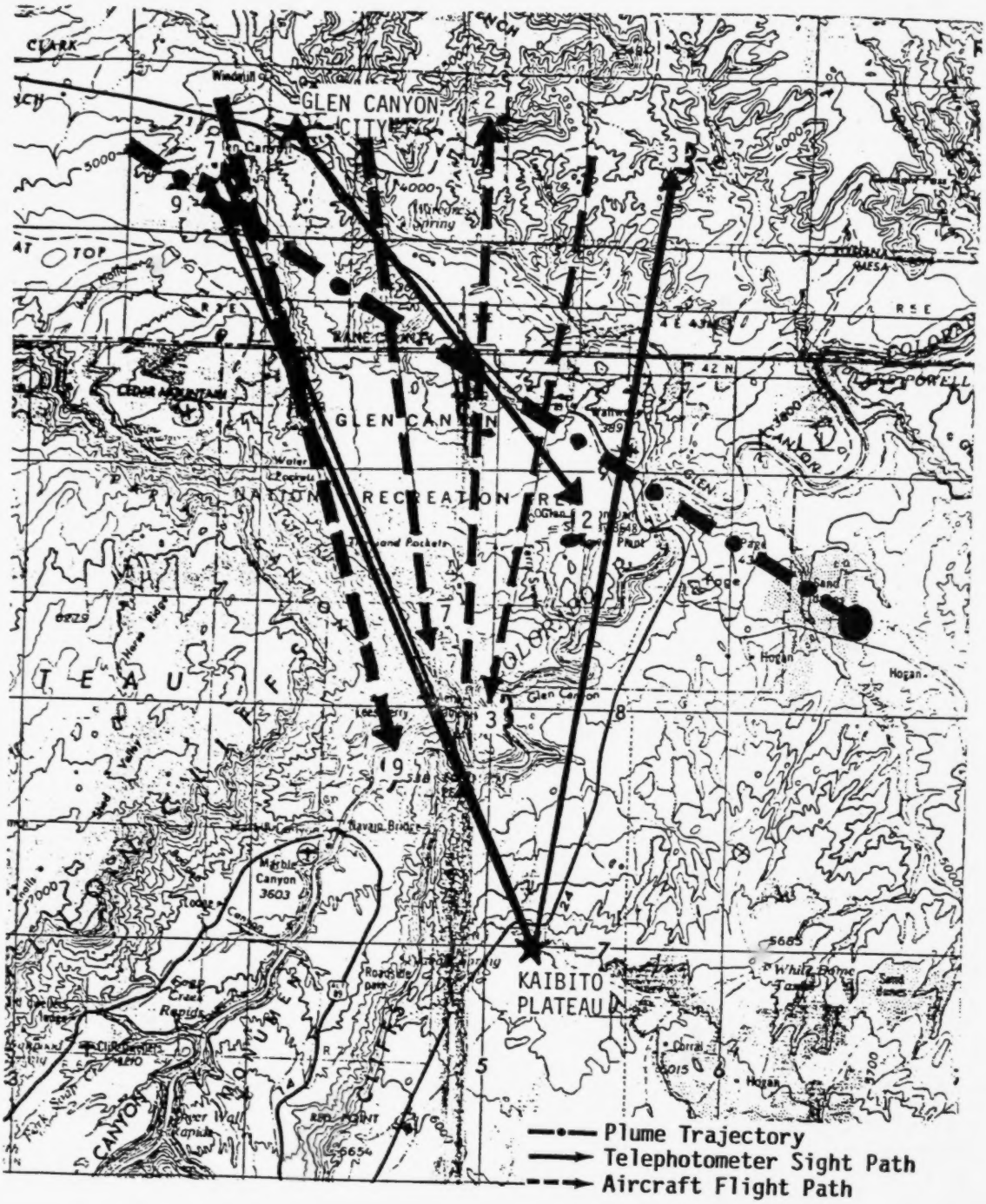

Figure 8. Case studies: December 15, 1979.

TABLE 8. INSTRUMENTATION USED IN VISTTA MEASUREMENTS

Measurement	Instruments	Estimated Level of Uncertainty
Primary emissions-- SO_2, NO_x, aerosols	Reported by the Salt River Project	See Table 9 of this report
NO/NO_x	Monitor Labs 8440 (MRI aircraft)	<10 ppb 5-10s time response to 90%
O_3	Monitor Labs 8410 (MRI aircraft)	5 ppb 5s time response to 90%
	Dasibi Model 1003-AH	5ppb
SO_2	Meloy 285 (MRI aircraft)	1 ppb 30s time response to 90%
b_{sp}	3-wavelength Integrating Nephelometer, University of Washington (MRI aircraft)	$<1 \times 10^{-6} m^{-1}$
Aerosol size distribution	TSI 3030 Royco 218/MCA Knollenberg ASSP Knollenberg ASASX-P (MRI aircraft)	Not characterized
	TSI 3030 Royco 220 Royco 245 (University of Minnesota)	Not characterized
Wind speed	Pilot balloons	Not characterized
Wind direction	From pilot balloon From airplane measurements of plume position	Not characterized <2 km time response to 90 % of SO_2 monitor < 30 sec; speed of aircraft = 70 m/sec^{-1}
Light intensity	Telephotometer MRI model 3010	See Bergstrom et al. (1982)

visibility model is not very sensitive to this content. One of the case studies was conducted with oxygen contents of 6.9 and 3 mole %, which was predicted to produce NO_2/NO_x ratios of 2.4 and 1.9% at the stack exit and 13.1 and 12.7% at 12 km downwind, respectively. The oxygen mole content that was measured on the simulated day was used in the data base when it was available. On days for which no measurements were performed (e.g., June 28, July 13, December 4, 1979), an average value, calculated from the measurements of the two programs, was used.

4.2.2.2 Emission Rates of Primary Pollutants

Emission rates of NO_x, SO_2, and total mass of primary particulates were measured in accordance with EPA reference test methods 1-7 by Energy and Environmental Resource Consultants. The size distribution of particulate emissions is discussed in Section 4.2.4.2 on aerosol data; the emission rate data are discussed in studies by Candelaria and Palomino (1982) and Richards et al. (1981b).

There is a large uncertainty in the emission rates of primary particulates for this study; for instance, emissions measured on December 7 1979 varied from 4.7 to 14.5 tons per day. However, at the NGS, visibility impairment is primarily caused by NO_2 absorption at the downwind distances considered.

The average emission rates and corresponding standard deviations are shown in Table 9. Average emission rates were calculated for each unit for each program (June-July and December 1979). When specific data were available for a unit, they were used in place of the average value.

4.2.3 Meteorological Data

Meteorological data such as wind speed, wind direction, and temperature profile are used in a plume visibility model to calculate plume dispersion and transport.

4.2.3.1 Wind Speed

Wind speed data were obtained from pilot balloons (MRI and SRP). For each case study, the wind speed measured at the altitude corresponding to the plume height was selected. Pilot balloons were released several times during a day of plume measurements, and the data measured at a time that corresponded most closely with the time of the telephotometer measurement were chosen.

TABLE 9. EMISSION RATES FOR THE NAVAJO GENERATING STATION FIELD PROGRAM--1979

Period	NO_x (kg hr^{-1})	SO_2 (kg hr^{-1})	Primary Aerosols (kg hr^{-1})
June-July			
Average emission rate	1374	3303	277
Standard deviation	173	138	130
December			
Average emission rate	1702	3448	194
Standard deviation	369	493	62

4.2.3.2 Wind Direction

Wind direction can also be calculated from pilot balloon data. However, the terrain is complex in the vicinity of NGS and variations in wind direction with time of day and altitude are important. Therefore, the plume trajectories were calculated from the aircraft measurements in the following manner: The maximum SO_2 concentration recorded by the aircraft was chosen as the plume centerline for each telephotometer measurement. Then, the plume trajectory was traced back to the source, and an effective wind direction was calculated. There is some uncertainty in this calculation because the time required to achieve a 90% response of the SO_2 monitor is on the order of 30 sec. Because the aircraft speed is about 70 $m.sec^{-1}$, this leads to a maximum uncertainty in the location of the SO_2 maximum on the order of 2 km. This method, however, gives more accurate results than are obtained using the pilot balloon data. The distance of the plume target downwind from the source is calculated from the geometry of the source location, plume trajectory, and telephotometer sight path.

4.2.3.3 Temperature

Temperature profiles were obtained several times daily from radio-sondes; the temperature sounding that corresponded to the time of the

telephotometer measurements was used. The Pasquill atmospheric stability classes were determined from the temperature profile at the calculated plume height. Table 10 shows the corresponding stability classes and temperature profile ranges.

4.2.3.4 Relative Humidity

Relative humidity was measured by the MRI aircraft, as well as at ground level at various times during the day.* A plume visibility model uses this value to calculate hydroxyl radical concentrations and the calculation of the hygroscopic growth of secondary aerosols. Because secondary aerosol formation had a negligible effect on plume visibility, relative humidity was not a major input variable.

4.2.4 Background Data

4.2.4.1 Trace Gas

Measurements of trace gas concentrations of NO, NO_x, SO_2, and O_3 in the background atmosphere were performed aloft by the MRI aircraft during both field programs and at ground level by the University of Minnesota

*Values used were obtained at plume height.

TABLE 10. PASQUILL STABILITY CLASS

Stability Class	Temperature Profile (°C/km)
A	$\lambda < -19$
B	$-19 < \lambda < -17$
C	$-17 < \lambda < -15$
D	$-15 < \lambda < -5$
E	$-5 < \lambda < 15$
F	$15 < \lambda < 40$

for the period of June-July 1979 and MRI for the month of December 1979. In this data base, the measurements made by the University of Minnesota were used for the June-July case studies and the measurements obtained in the background by the MRI aircraft were used for the December case studies. The University of Minnesota ground-level monitoring station was located at Zilnez Mesa at an elevation of 2286 m.msl, which corresponds roughly to the plume height. These measurements are thus representative of background concentrations at plume height. Ozone concentrations varied from 33 to 44 ppb. A plume visibility model is fairly sensitive to background ozone concentrations (Johnson, 1980) because NO_2 formation in the plume is formed primarily from the reacton of NO with O_3. Hydrocarbon concentrations were measured during the June-July program (Sheppard et al. 1980), but no aldehyde concentrations were available. Model calculations have shown that OH concentrations are sensitive to hydrocarbon concentrations and particulary to aldehyde concentrations (Seigneur, 1982).

4.2.4.2 Aerosol Data

In the EPA/SAI plume visibility model, the aerosol populations are represented by two log-normal distributions that characterize the accumulation mode and the coarse mode. Two aerosol populations are input into the model, one for the background and one for the plume. These log-normal aerosol population distributions are characterized by mean radius, standard deviation, and aerosol density. A common data set, characteristic of the VISTTA data, was chosen for all case studies.

The aerosol concentrations in the plume are determined from the emission data and the aerosol growth calculations. Secondary aerosol growth was negligible for the case studies considered. The background aerosol concentration was defined from the visual range. Aerosol distribution data were collected at the stacks, in the background air, and in the plume at various locations aloft and at ground level. The references used in the definition of the aerosol distributions are listed in Section 4.3. An aerosol distribution representative of clean air conditions was used for all simulations because no forest fires or urban plume affected background conditions on the day considered. Day-specific aerosol distributions are available from MRI or STI.

4.2.4.3 Nephelometer Measurements

Nephelometer measurements were carried out at ground-level sites and aloft. The measured particulate scattering coefficients were used along with a calculated Rayleigh coefficient to compute the visual range. Nephelometer data obtained in the background air by the MRI aircraft were used for these calculations. For each set of data (e.g., December 7 morning data), an

average particulate scattering coefficient was calculated. Because some particles can impact in the tubing before entering the nephelometer, the scattering coefficient could be too low; that is, the computed values of the visual range could be slightly high.

4.2.5 Measurements of Plume Characteristics

4.2.5.1 Plume Visual Effects--Ground-Based Measurements

Telephotometer measurements were performed from several ground-level sites to evaluate the plume visual effect at four wavelengths--405, 450, 550, and 630 nm. The computation of plume contrast from telephotometer measurements has been described by Bergstrom et al. (1982). The main difficulty with the telephotometer measurements performed for this study was that the adjustments and recording of the data were done manually and took several minutes. Comparison of telephotometer measurements of the same plume target, performed at five-minute time intervals, showed that there was an uncertainty in measurements of plume contrast of about 20% for contrasts on the order of 0.10. Larger uncertainties in measurements could exist for low contrast values or for cases in which the plume is at the horizon.

4.2.5.2 Aircraft Measurements of the Plume

Data on plume width and plume concentrations of NO, NO_2, and SO_2, and particulates are useful for evaluating the dispersion and chemistry modules of a plume visibility model. The plume widths were calculated from the recorded SO_2 concentrations above 20 ppb. There could be some uncertainty in this value caused by the time response of the SO_2 monitor (30 sec to achieve a 90% response). Corrections were made for cases in which the aircraft flight path made an angle with the crosswind direction.

Maximum plume concentrations are given for NO, NO_2, and SO_2. Integrated concentrations of NO_2 and particulates--or alternatively, particulate scattering coefficients at 450 nm, b_{sp} (450)--are of special interest in a plume visibility model evaluation because they are directly related to the visual effect of the plume. These integrated concentrations have been calculated from the mean plume values of NO_2 and b_{sp} (450) and have been corrected for the angle of the flight path and the crosswind direction; they correspond to the crosswind integrated values. Continuous measurements of plume concentrations were made during the flights; these crosswind concentration profiles are available from MRI or STI.

4.2.6 Additional Data for Optics Component Evaluation

The evaluation of the optics component of a visibility model requires the following data:

> Data on the geometry of the sun, observer, and plume positions.

> The plume burden (NO_2 and particulate concentrations along the sight path).

> The value of the visual range.

In this section, we summarize the development of this data base from the raw data. The plume-observer geometry is determined from the plume trajectory, the source location, the observer location and the measured plume height; the sun position is determined from the time of the day; and the scattering angle can be deduced simply from the sun-plume-observer geometry. This is shown schematically in Figure 9.

The plume width was determined from the SO_2 concentrations above 20 ppb. It was corrected by the angle between the flight path and plume direction so that the listed plume width corresponded to the actual crosswind plume width. (As mentioned in the previous subsection, uncertainty exists for this measurement because of the time response of the SO_2 monitor.) The average concentrations of NO_2 and particle scattering coefficients at 550 nm, $b_{sp}(550)$, were calculated from aircraft measurements along the flightpath in the plume. The integrated crosswind NO_2 concentration and $b_{sp}(550)$ values were obtained by simple multiplication of these mean plume values by the plume width.

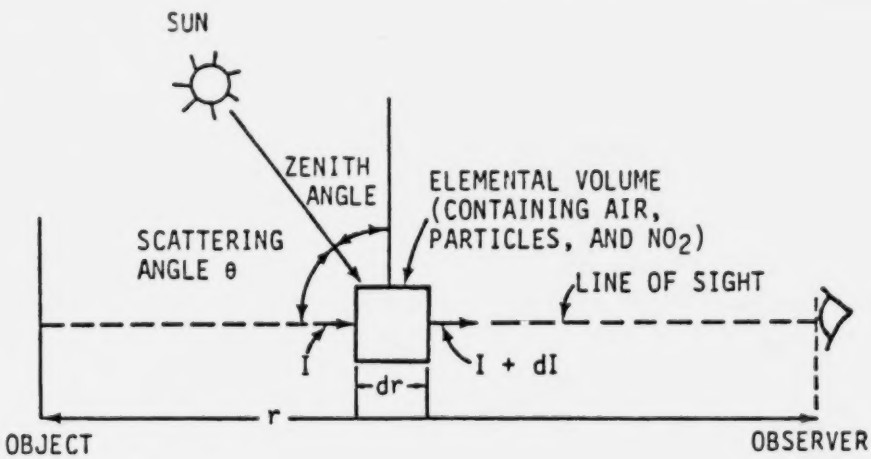

Figure 9. Schematic representation of sun-plume-observer geometry.

Note that the integral values in the plume for NO_2 and b_{sp} are along the crosswind direction and not along the sight path; thus, these values must be corrected by the angle between the sight path and the crosswind direction to be input into the optics component. The value of $b_{sp}(550)$ could be slightly underestimated because of the impact of some particulates on the tubing before entering the nephelometer. The value of b_{sp} at other wavelengths can be easily calculated from the value at 550 nm and from the aerosol distribution. The visual range is deduced from nephelometer measurements of the particulate scattering coefficient at 550 nm and, as just mentioned, could be slightly overestimated because of the underestimation of $b_{sp}(550\ nm)$.

4.3 DATA BASE FOR PLUME VISIBILITY MODEL EVALUATION

This section presents 27 case studies of plume visibility model evaluation for three different levels of data:

- Data common to all case studies.
- Data common to a particular set of case studies, i.e., day or half-day studies.
- Data specific to a case study that involves both input and model evaluation data.

The presentation of this data base is summarized in Table 11. The different levels of data are presented in Tables 12 and 13. An overview of those VISTTA case studies selected for plume visibility model evaluation is shown in Figure 10.

Temperature profiles for each set of case studies are shown in Figures 11 through 16. Temperature lapse rates are given at the plume height estimated from aircraft data. The solar zenith, azimuth angle, and scattering angle were calculated from the time and location data. Background aerosol concentration (coarse mode and submicron (sulfate) aerosol) were calculated by EPA/SAI plume visibility model from the visual range and are not measured data. In this calculation, it is assumed that the accumulation mode contributes two thirds of the overall particulate scattering coefficient; the coarse mode contributes one third.

The plume width and integrated plume concentrations, i.e., NO_2 and $b_{sp}(550\ nm)$, were corrected for the angle between the flight path and the crosswind direction. Thus, the values presented (plume width and integrated plume concentrations) are along the crosswind direction.

TABLE 11. SUMMARY OF KINDS OF DATA COLLECTED DURING THE EPA/VISTTA 1979 FIELD PROGRAMS

Data Common to All Case Studies	
> Source characteristics	= Location, number of stacks, stack height
> Aerosol characteristics	= Log-normal distributions, particle densities
Data Common to a Set of Case Studies (Day or Half-Day)	
> Date	
> Source characteristics	= Emission rates, flue gas characteristics
> Meteorological data	= Temperature profile, atmospheric stability, mixing height
> Optics data	= Visual range, background conditions
Data Specific to a Case Study	
Input Data:	
> Observer data	= Time, location, plume target
> Meteorological data	= Wind speed, wind direction, temperature, relative humidity
> Trace gas data	= Background ozone, nitric oxide, nitrogen dioxide, and sulfur dioxide concentrations
Model Evaluation Data:	
> Telephotometer measurements	= Plume contrast at 4 wavelengths
> Plume measurements	= Plume width, plume concentrations

TABLE 12. DATA COMMON TO ALL CASE STUDIES

Source Characteristics (Navajo Generating Station):

Source Location (UTM Coordinates)

Easting: 464.8 km

Northing: 4084.0 km

Elevation: 1328.9 m msl

Number of Stacks: 3

Stack Height: 236 m (1565 m msl)

Emissions Characteristics

	June 28, July 13	December 4	December 7	December 5
SO_2 (TPD)	261.9	273.03	177.12	286.71
NO_x (TPD)	108.93	127.67	97.39	124.72
Particulates (PTD)	21.96	16.07	8.43	18.04
Units operating	3	3	2	3
O_2mole%	6.6	6.6	6.9	6.2
Temperature °F	300	300	300	300
Flow (m^3/s)	1491	1491	1491	1491
Exit velocity (m/s)	27.0	27.0	27.0	17.0

Telephotometer Sites

	UTM Coordinates		Elevation
	East	North	m, msl
Kaibito Plateau	451.7	4070.2	1681.0
Lechee Rock	475.7	4073.0	1645.9
Kaibito City	495.1	4053.0	1786.1
Glen Canyon City	441.1	4104.5	1219.2

TABLE 12 (concluded)

Aerosol Characteristics:

	Background		Plume	
	Accumulation mode	Coarse mode	Accumulation mode	Coarse mode
Mass Median Radius (μm)	0.125[*]	3.000[†]	0.125[±]	1.750[**]
Standard Geometric Deviation	1.600[#]	2.200[†]	1.600[#]	2.500[**]
Particle Density (g/cm^3)	1.800	2.000	1.800	2.000

Index of Refraction: 1.5 + 0.0 i

[*] Hering, S. V. (1981).

[†] Whitby, K. T. and G. M. Sverdrup (1978).

[±] Richards, L. W. et al. (1981b).

[**] Candelaria, R. B. and G. E. Palomino (1980).

[#] McMurry, P. H. (1980).

TABLE 13. 1979 VISTTA CASE STUDIES

Date	June 28 1979		July 13 1979		December 4 1979					December 7 Morning 1979							
MRI Tape/Pass	67/5	67/7	82/1	82/1	91/2	91/3	91/4	91/5	91/12	94/2	94/3	94/4	94/7	94/8	94/9	94/10	94/11
Photographic Slide Number	1	2	3	4	5	6	7	8	9	10	11	12	13	14	15	16	17
Meteorological Data (Plume height)																	
Wind direction (degrees)	290.0	246.0	295.0	295.0	81.0	81.0	85.0	99.0	123.0	99.0	90.0	79.0	96.0	99.0	94.0	128.0	89.0
Wind speed ($m.sec^{-1}$)	1.3	3.6	3.0	3.0	1.5	1.5	1.7	2.5	2.6	2.0	2.0	2.0	2.0	2.0	2.0	2.0	2.0
Temperature (°F)	78.8	78.8	77.0	77.0	52.8	52.8	52.8	52.8	52.8	40.0	42.0	42.0	50.0	50.0	50.0	50.0	50.0
Relative humidity (%)	45.0	45.0	16.0	16.0	45.0	45.0	45.0	45.0	67.0	60.0	60.0	60.0	55.0	55.0	55.0	55.0	55.0
Optics Data (Telephotometer Site)																	
Downwind distance at which plume is observed:(km)	11.5	28.0	28.7	28.7	9.25	16.5	19.5	24.75	15.0	21.25	21.25	11.75	20.8	21.5	14.0	9.3	4.3
Time (MST)	0726	0845	0706	0707	0934	0951	1008	1042	1241	0908	0929	0949	1030	1044	1107	1135	1154
Solar zenith angle (degrees)	65.2	49.5	70.4	70.2	70.3	68.3	66.4	63.2	59.5	74.3	71.5	69.0	64.6	63.3	61.8	60.4	59.8
Solar azimuth angle (degrees)	78.6	89.5	76.9	77.0	140.4	144.0	147.7	155.6	186.8	135.2	139.4	143.5	152.6	156.0	161.6	168.8	173.8
Plume centerline-observer distance (km)	26.2	46.2	15.1	19.4	13.1	11.7	13.9	21.2	22.0	18.9	16.0	11.7	17.7	19.0	14.8	20.4	16.3
Azimuth of line of sight (degrees)	68.3	56.9	94.1	347.0	18.8	341.7	330.5	326.8	1.4	335.3	329.4	7.7	334.6	334.6	356.6	16.5	32.7
Elevation angle of line of sight (degrees)	0.8	0.3	1.4	0.6	0.8	0.9	0.7	0.4	0.4	0.8	0.9	1.3	0.9	0.8	1.0	0.7	0.9
Scattering angle (degrees)	26.7	50.2	25.8	90.0	119.6	152.3	144.9	151.9	149.1	154.7	159.1	132.0	154.5	153.3	148.4	140.3	132.3
Angle to plume centerline (degrees)	41.7	9.1	20.9	52.0	62.2	80.7	65.5	47.8	58.3	56.3	59.4	71.3	58.6	55.6	82.6	68.5	56.3
Visual range (km) from nephelometer (550 nm)	177	177	184	184	228	228	228	228	292	292	292	292	292	292	292	292	292
Telephotometer Measurements - Site	KP	KP	LR	KC	KP	KP	KP	KP	KP	KP	KP	KP	KP	KP	KP	KP	KP
Plume/Background intensity at:																	
405 nm	0.950	1.20	0.875	0.935	0.88	0.86	0.88	0.86	0.89	0.933	0.925	0.894	0.902	0.89	0.873	0.90	0.819
450 nm	0.963	1.26	0.895	0.945	0.87	0.86	0.83	0.85	0.90	0.905	0.926	0.915	0.899	0.876	0.905	0.881	0.779
550 nm	1.076	1.41	0.980	0.995	0.94	0.95	0.90	0.96	0.97	0.939	0.942	0.934	0.942	0.935	0.942	0.927	0.860
650 nm	1.103	1.50	1.03	0.995	0.98	0.98	0.98	0.96	0.97	0.969	0.973	0.946	0.985	1.0	0.988	0.979	0.959
Plume Measurements (Aircraft)																	
Aircraft downwind distance	(Same as telephotometer downwind distance, except Dec. 15 Passes 3,7,9 →																
Plume Width (km)	0.52	7.8	3.7	3.7	12.10	9.34	6.79	8.53	18.1	1.86	6.3	2.9	5.1	4.95	2.75	7.56	7.74
Plume Altitude (centerline) m msl	1876	1853	2208	2208	1966	1957	1924	1949	1910	2011	2057	1960	2028	2023	2006	2026	2031
Maximum plume concentrations																	
NO (ppm)	0.073	0.108	0.231	0.231	>FS	0.681	0.374	0.104	0.421	0.186	0.207	0.602	0.907	1.169	0.564	1.104	0.657
NO_2 (ppm)	0.049	0.061	0.051	0.051	>FS	0.085	0.053	0.040	0.062	0.031	0.044	0.096	0.114	0.119	0.072	0.111	0.064
SO_2 (ppm)	0.194	0.284	0.430	0.430	>FS	1.044	0.588	0.216	0.804	0.105	0.157	0.534	1.127	1.291	0.311	1.408	1.196
Plume Characteristics (Aircraft)																	
Plume concentrations integrated along the crosswind direction																	
$\int NO_2\ dy$ (ppm-km)	0.015	0.268	0.130	0.130	-	0.335	0.288	0.294	0.803	0.041	0.148	0.065	0.165	0.146	0.048	0.281	0.227
$\int b_{sp}(450)\ dy$	0.011	0.161	0.085	0.085	0.384	0.182	0.147	0.149	0.486	0.016	0.086	0.064	0.117	0.101	0.051	0.209	0.192
$\int b_{sp}(550)\ dy$	0.009	0.127	0.073	0.073	0.349	0.145	0.119	0.113	0.400	0.014	0.084	0.062	0.122	0.102	0.047	0.211	0.199
$\int b_{sp}(630)\ dy$	0.007	0.098	0.067	0.067	0.341	0.127	0.108	0.095	0.356	0.014	0.085	0.064	0.131	0.107	0.048	0.230	0.217
Trace Gas Background Concentrations																	
NO_x (ppm)	NO_x concentrations in background negligible.																
NO_2 (ppm)	NO_2 "				"												
O_3 (ppm)	0.034	0.034	0.044	0.044	0.044	0.034	0.034	0.034	0.034	0.031	0.034	0.036	0.034	0.035	0.034	0.035	0.033
SO_2 (ppm)	SO_2 below minimum detectable levels.																
Aerosol Background Concentrations																	
Coarse mode ($\mu g \cdot m^{-3}$)	3.6	3.6	3.6	3.6	3.6	3.6	3.6	3.6	3.6	3.6	3.6	3.6	3.6	3.6	3.6	3.6	3.6
Sulfate ($\mu g \cdot m^{-3}$)	3.9	3.9	4.3	4.3	2.3	2.3	2.3	2.3	2.3	0.8	0.8	0.8	0.8	0.8	0.8	0.8	0.8

TABLE 13 (concluded)

Date	December 7-Afternoon-1979 1979						December 15 1979 1979				Comments
MRI Tape/Pass	95/1	95/2	95/3	95/4	95/5	95/7	103/2	103/3	103/7	103/9	
Photographic Slide Number	18	19	19	20	20	21	22	23	24	25	Slides are available from MRI: $100/set purchase; $25 loan, handling.
Meteorological Data (Plume height)											
Wind direction (degrees)	103.0	103.0	81.0	91.0	127.0	123.0	122.0	123.0	122.0	122.0	
Wind speed ($m.sec^{-1}$)	2.4	2.4	2.41	2.4	2.4	2.0	2.6	2.6	2.6	2.6	
Temperature (°F)	52.8	52.8	52.8	52.0	52.0	49.0	42.0	42.0	44.0	43.0	
Relative humidity (%)	36.0	36.0	36.0	45.0	45.0	54.0	31.0	32.0	27.0	29.0	
Optics Data (Telephotometer Site)											
Downwind distance (km)	7.75	12.0	12.5	17.0	22.5	22.0	17.7	11.5	30.5	31.3	
Time (MST)	1409	1427	1438	1459	1505	1540	1125	1133	1209	1236	
Solar zenith angle (degrees)	65.1	66.9	68.2	70.7	71.5	76.3	61.6	61.2	60.3	60.3	
Solar azimuth angle (degrees)	206.6	212.6	215.0	219.4	220.6	227.1	165.5	167.5	176.9	184.1	
Plume centerline-obs. dist. (km)	16.5	16.6	11.9	11.5	27.8	26.3	14.1	20.2	32.6	33.2	
Azimuth of line of sight (degrees)	19.6	4.9	3.6	344.5	349.9	348.1	142.0	9.6	336.9	336.1	
Elevation angle (degrees)	0.8	0.8	1.1	0.9	0.5	0.5	2.4	0.4	0.3	0.3	
Scattering angle (degrees)	154.2	144.5	142.4	122.9	126.9	120.0	36.2	144.3	144.7	140.1	
Angle to plume centerline (degrees)	83.4	81.9	77.4	73.5	42.9	45.3	20.0	67.6	34.9	34.1	
Visual range (km) (550 nm)	274	274	274	274	274	274	260	260	260	260	
Telephotometer Measurements - Site	KP	KP	KP	KP	KP	KP	GC	KP	KP	KP	KP = Kaibito Plateau LR = Lechee Rock KC = Kaibito City GC = Glen Canyon City
Plume/Background intensity at:											
405 nm	0.830	0.83	0.851	0.848	0.940	0.773	0.882	0.758	0.819	0.806	
450 nm	0.844	0.810	0.818	0.819	0.940	0.777	0.893	0.887	0.837	0.828	
550 nm	0.925	0.925	0.919	0.925	0.930	0.863	0.991	0.951	0.920	0.883	
650 nm	0.969	0.975	0.981	0.983	1.0	0.976	0.937	0.984	0.962	0.969	
Plume Measurements (Aircraft)											
Aircraft downwind distance	(Same as telephotometer distance →						15.5	23.3	30.3		
Plume Width (km)	8.66	9.22	8.5	0.5	1.19	13.0	10.92	11.1	8.26	15.7	
Plume Altitude (centerline)	1951	1876	1864	1907	1957	1808	1938	1942	1966	1931	
Maximum plume concentrations											
NO (ppm)	0.347	0.193	0.165	0.031	0.024	0.177	>FS	1.312	0.664	0.373	>FS = readings greater than full scale on instrument.
NO_2(ppm)	0.046	0.045	0.044	0.013	0.020	0.046	>FS	0.104	0.122	0.084	
SO_2(ppm)	0.444	0.246	0.239	0.026	0.035	0.266	>FS	1.722	1.103	0.484	
Plume Characteristics (Aircraft)											
Plume concentrations integrated along the crosswind direction											
$\int NO_2\, dy$ (ppm-km)	0.234	0.248	0.226	0.007	0.020	0.359	-	0.386	0.298	0.169	To find plume concentration along sight path, divide these values by sin(angle to plume centerline).
$\int b_{sp}(450)\, dy$	0.106	0.108	0.092	0.003	0.008	0.132	0.482	0.284	0.204	0.217	
$\int b_{sp}(550)\, dy$	0.099	0.099	0.085	0.002	0.007	0.117	0.482	0.270	0.185	0.189	
$\int b_{sp}(630)\, dy$	0.098	0.098	0.085	0.002	0.006	0.117	0.494	0.269	0.183	0.176	
Trace Gas Background Concentrations											
NO_x (ppm)											
NO_2 (ppm)											
O_3 (ppm)	0.034	0.034	0.034	0.035	0.037	0.033	0.038	0.038	0.038	0.037	
SO_2 (ppm)											
Aerosol Background Concentrations											
Coarse mode ($\mu g \cdot m^{-3}$)	3.6	3.6	3.6	3.6	3.6	3.6	3.6	3.6	3.6	3.6	Estimated; this value used in modeling.
Sulfate ($\mu g \cdot m^{-3}$)	1.5	1.5	1.5	1.5	1.5	1.5	1.8	1.8	1.8	1.8	

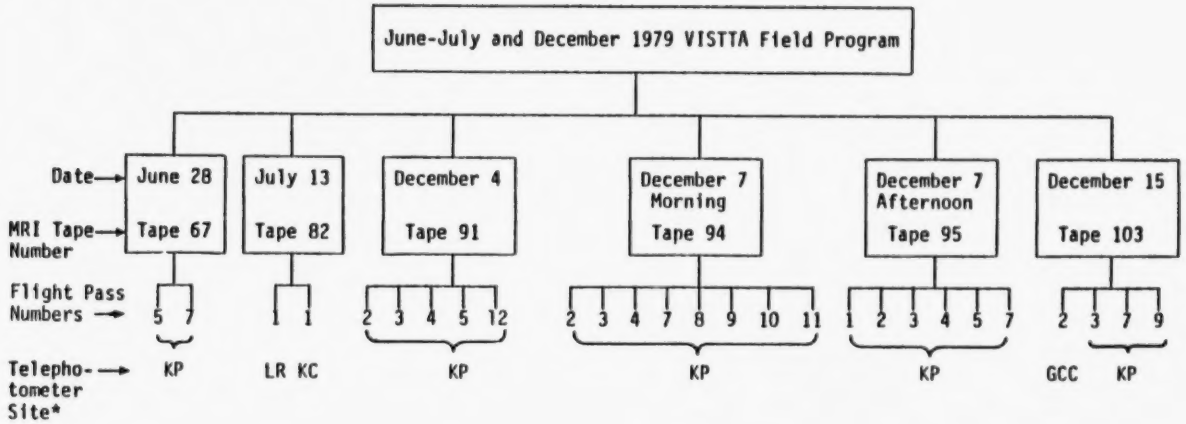

* KP = Kaibito Plateau; LR = Lechee Rock; KC = Kaibito City; GCC = Glen Canyon City

Figure 10. Case studies for plume visibility model evaluation.

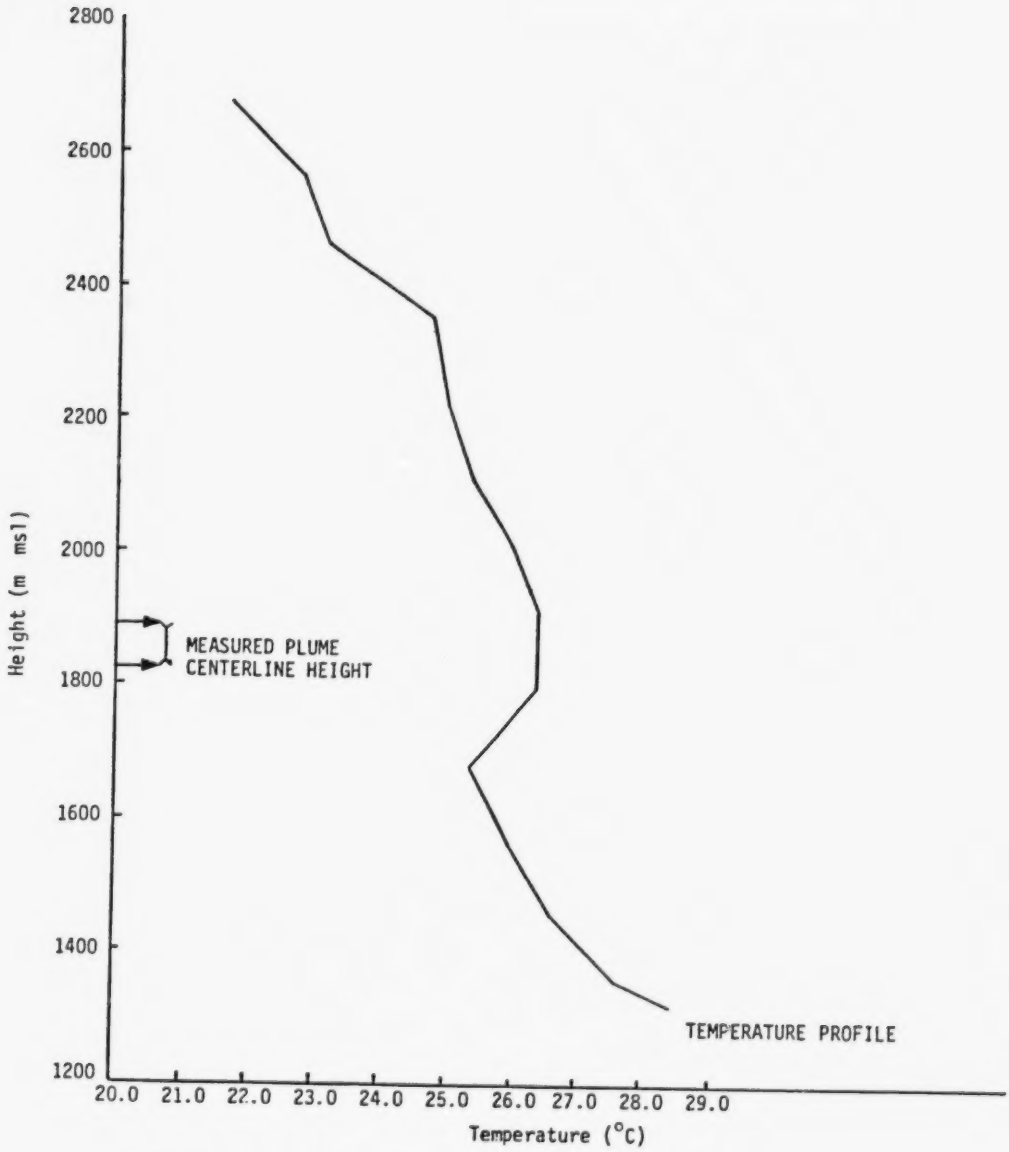

Figure 11. Temperature profile for the case study of June 28, 1979 at 0900 MST.

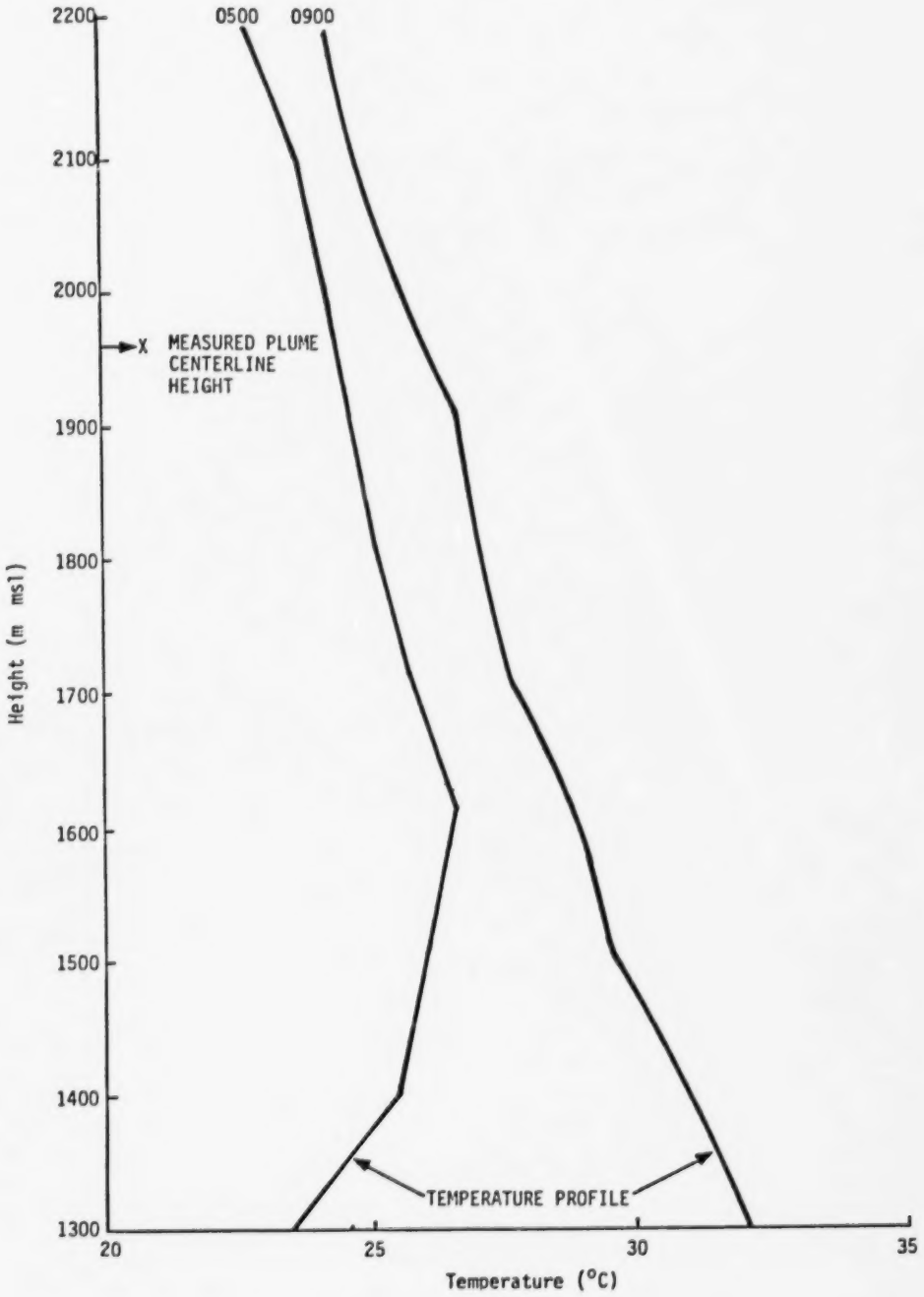

Figure 12. Temperature profile for the case study of July 13, 1979 at 0500 and 0900 MST.

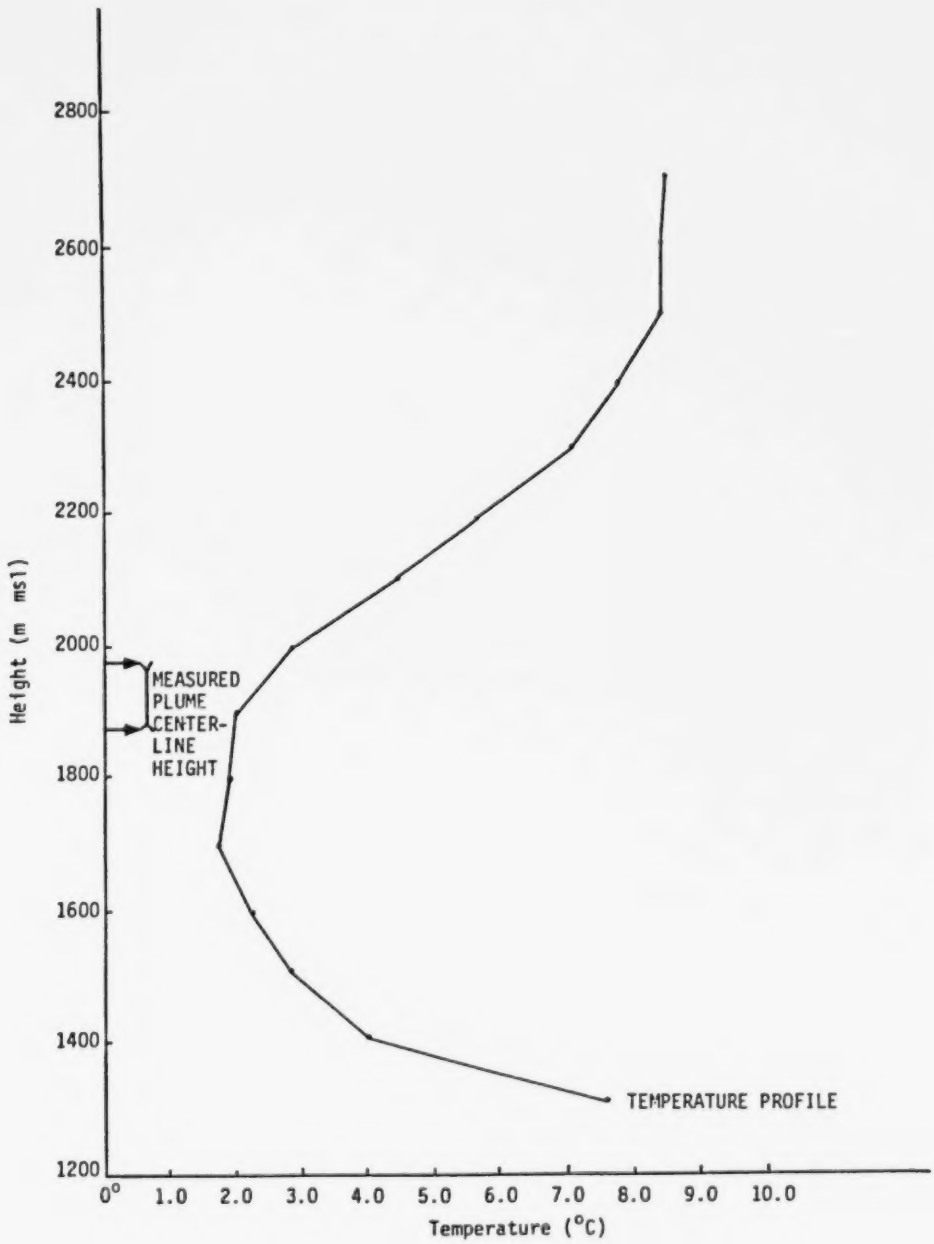

Figure 13. Temperature profile for the case study of December 4, 1979 at 0856 MST.

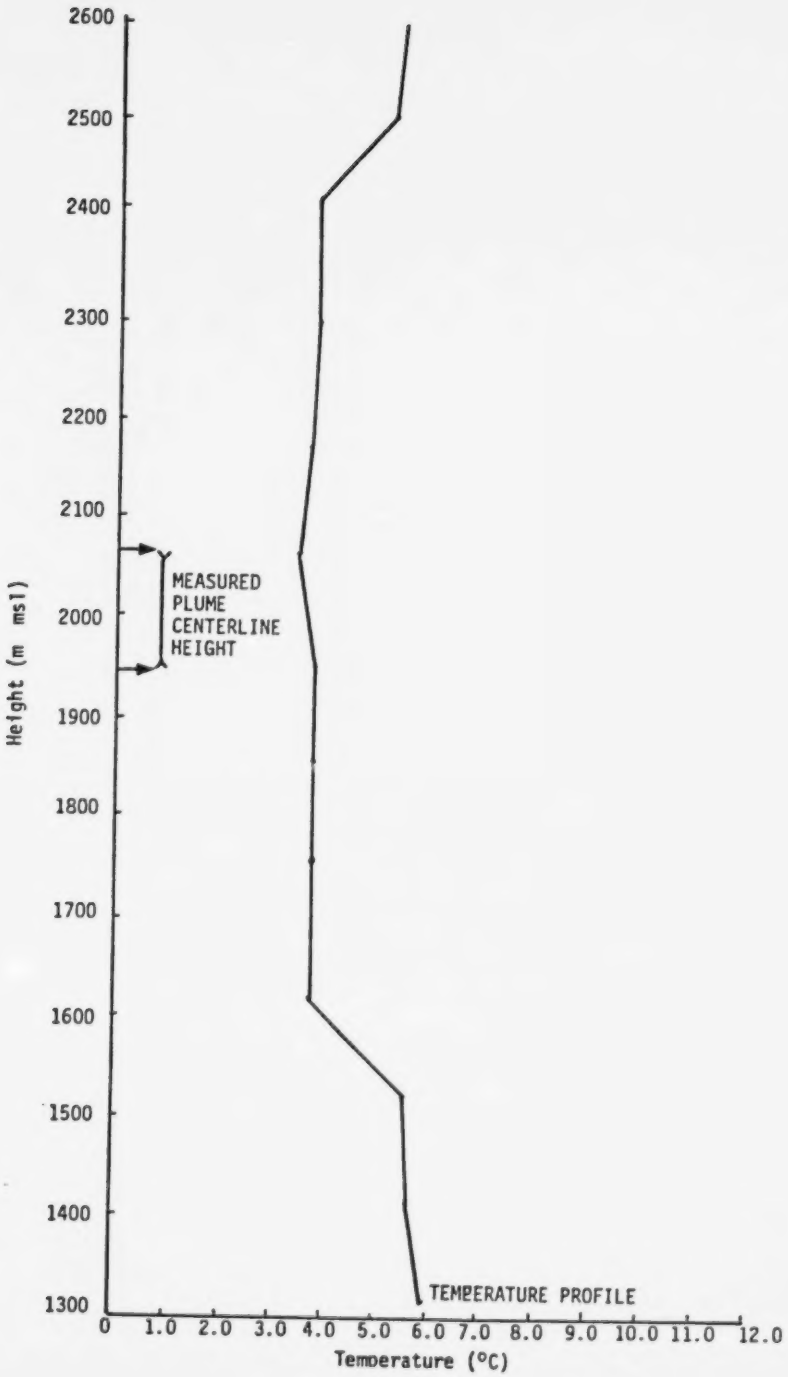

Figure 14. Temperature profile for the case study of December 7, 1979 at 0847 MST.

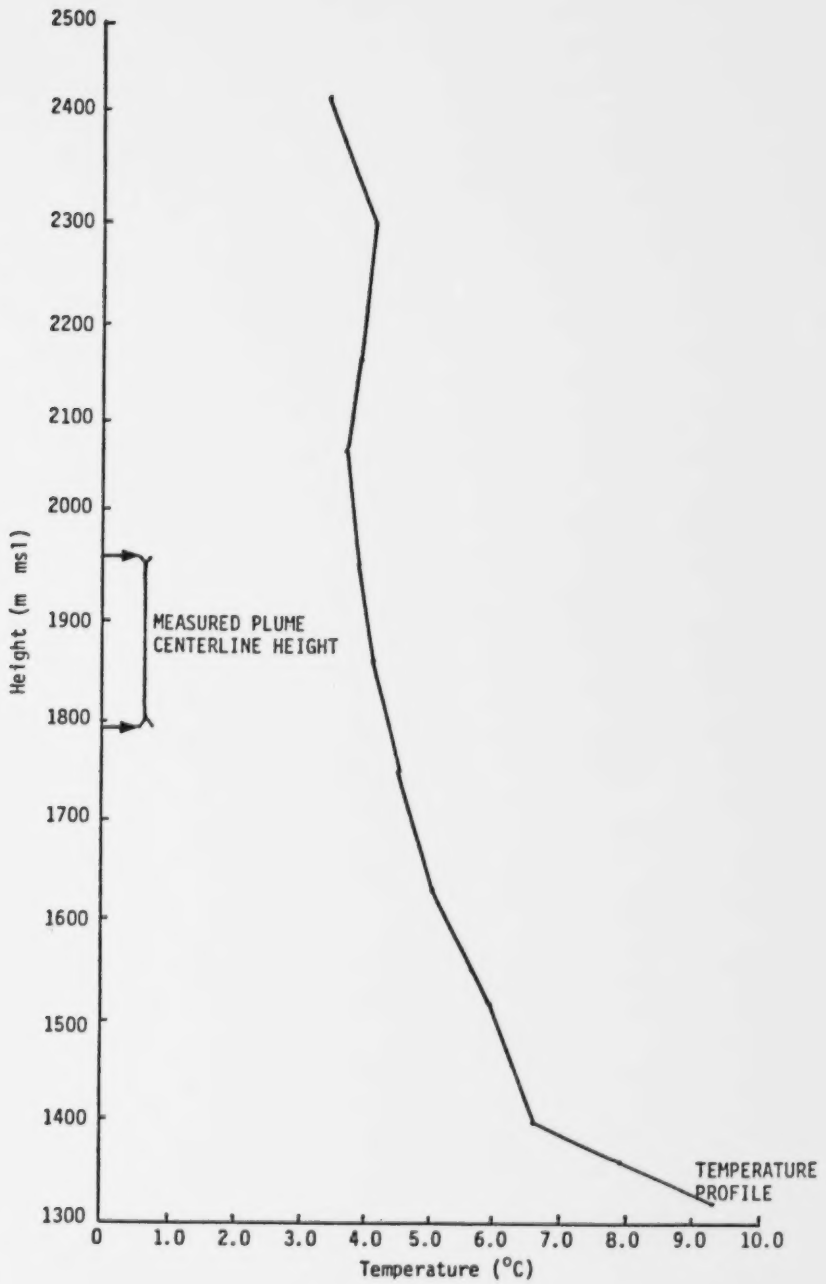

Figure 15. Temperature profile for the case study of December 7, 1979 at 1248 MST.

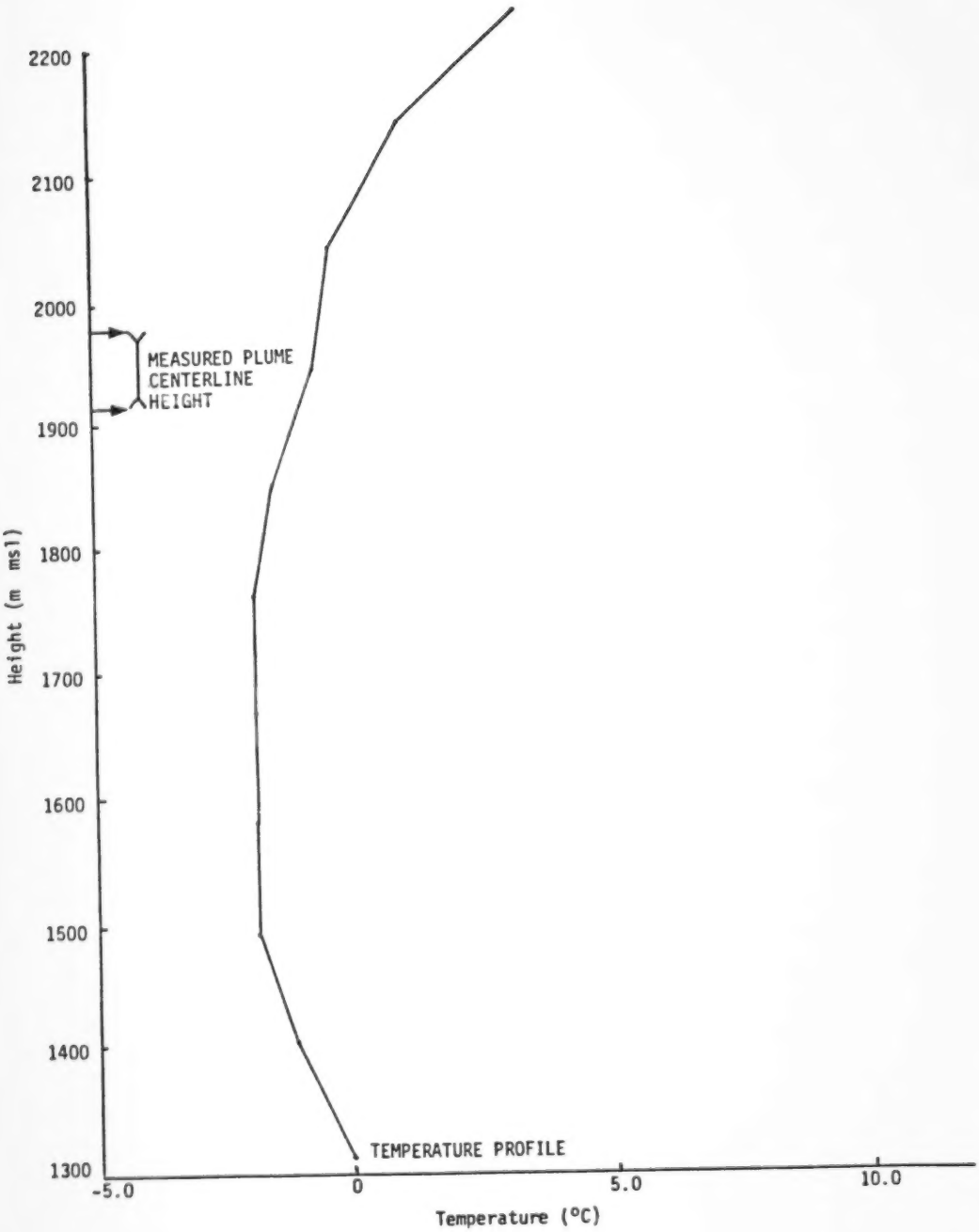

Figure 16. Temperature profile for the case study of December 15, 1979 at 0845 MST.

It should be noted that in some cases the aircraft very likely did not fly through the plume center, but through the plume top or bottom edges. In these cases, plume concentrations and plume widths are lower than would be expected from the measurements obtained from other case studies of the same day. This is probably true for cases two and nine on the morning of December 7 1979 and cases four and five on the afternoon of December 7 1979.

REFERENCES

Babson, B. L., R. W. Bergstrom, M. A. Samuelson, C. Seigneur, A. Waggoner, and W. C. Malm (1982) Statistical Analysis of Nephelometer Regional Field Data. Atmos. Environ. 16, 2335-2346.

Bergstrom, R. W., C. Seigneur, B. L. Babson, H-Y. Holman, and M. A. Wojcik (1981) Comparison of the Observed and Predicted Visual Effects Caused by Power Plant Plumes. Atmos. Environ. 15, 2135-2150.

Bergstrom, R. W., W. D. Jensen, K. O'Dell, W. C. Malm, and M. Gannon (1982) Calibration and Error Analysis of Multiwavelength Telephotometers. Atmos. Environ. 16, 2735-2743.

Bhardwaja, P. S., D. W. Moon, and G. L. Powell (1981) Visibility Trends in the Vicinity of an Isolated Power Plant. Atmos. Environ. 15, 1943-1953.

Cahill, T. A., B. H. Kusko, L. L. Ashbaugh, J. B. Barone, R. A. Eldred, and E. G. Walther (1981) Regional and Local Determinations of Particulate Matter and Visibility in the Southwestern United States during June and July, 1979. Atmos. Environ. 15, 2011-2016.

Candelaria, R. B. and G. E. Palomino (1982) Characterization of Navajo Generating Station Emissions Measured during the June-July 1979 VISTTA Field Program. Atmos. Environ. 16, 2287-2298.

Flagan, R. C. and D. D. Taylor (1980) Aerosols from a Laboratory Pulverized Coal Combustor. Proc. Second Chemical Congress of the North American Continent, Las Vegas, Nevada, August 24-29, ACS Annual Conference.

Friedlander, S. K. (1980) Fine Aerosols of the Southwest: Implications for Fundamental Research. Ann. N.Y. Acad. Sci. 6, 588-598.

Hering, S. V., J. L. Bowen, J. G. Wengert, and L. W. Richards (1981) Characterization of the Regional Haze in the Southwestern United States. Atmos. Environ. 15, 1999-2009.

Hogo, H. C., C. Seigneur, and R. W. Bergstrom (1981) Coal-Fired Power Plant Contribution to Visibility Impairment in Western Pristine Areas: Telephotometer Measurements--Processed Data--Documentation. 7-ES81-26, Systems Applications, Inc., San Rafael, California.

Horvath, H. (1981) The University of Vienna Telephotometer. Atmos. Environ. 15, 2537-2546.

Hudischewskyj, A. B., B. L. Babson, R. W. Bergstrom, and C. Seigneur (1981) Coal-Fired Power Plant Contribution to Visibility Impairment in Western Pristine Areas: Index to the Photographs Taken from Telephotometer Sites during the June-July and December 1979 VISTTA Field Programs. 6-ES81-25, Systems Applications, Inc., San Rafael, California.

Johnson, C. D. (1980) Sensitivity Analysis of the Plume Visibility Model (PLUVUE), Systems Applications, Inc., San Rafael, California.

Johnson, C. D., D. A. Latimer, R. W. Bergstrom, and H. Hogo (1980) User's Manual for the Plume Visibility Model (PLUVUE). Systems Applications, Inc. Final Report 28-ES80-160R, to U.S. Environmental Protection Agency, Contract 68-02-3337.

Macias, E. S., D. L. Blumenthal, J. A. Anderson, B. K. Cantrell (1979) Characterization of Visibility Reducing Aerosols in the Southwestern United States: Interim Report on Project VISTTA. MRI 78 IR-1585, Meteorology Research, Inc., Altadena, California.

Macias, E. S., D. L. Blumenthal, J. A. Anderson, and B. K. Cantrell (1980) Size and Composition of Visibility-Reducing Aerosols in Southwestern Plumes. Ann. N.Y. Acad. Sci. 338, 233.

Macias, E. S., J. O. Zwicker, J. R. Ouimette, S. V. Hering, S. K. Friedlander, T. A. Cahill, G. A. Kuhlmey, and L. W. Richards (1981a) Aerosol Chemical Composition in the Southwestern U.S. Atmos. Environ. 15, 1971-1986.

Macias, E. S., J. O. Zwicker, and W. H. White (1981b) Source Contributions to Regional Haze in the Southwestern U. S. Atmos. Environ. 15, 1987-1997.

Markowski, G. R., D. S. Ensor, R. G. Hopper, and R. C. Carr (1980) A Submicron Aerosol Mode in Flue Gas from a Coal Utility Boiler. Environ. Sci. & Technol. 14, 1400-1402.

McMurry, P. H., N. E. Valentine, A. J. Kelly (1980) Data Report, University of Minnesota Mobile Laboratories. VISTTA Project, Zilnez Mesa; June-July 1979. Particle Technology Laboratory Publication No. 414. University of Minnesota, Minneapolis, Minnesota.

McMurry, P. H., D. J. Rader, and J. L. Stith (1981) Growth Laws for Secondary Aerosols in Power Plant Plumes: Implications for Chemical Conversion Mechanisms. Atmos. Environ. 15, 2315-2327.

Ogren, J. A., D. L. Blumenthal, W. H. White, T. W. Tesche, M. A. Yocke, and M. K. Liu (1976) Determination of the Feasibility of Ozone Formation in Power Plant Plumes. Meteorology Research, Inc. and Systems Applications, Inc., Electric Power Research Institute Report EA-307. Menlo Park, California.

Ogren, J. A., D. L. Blumenthal, and A. H. Vanderpol (1977) Oxidant Measurements in Western Power Plant Plumes. Electric Power Research Institute Report. EA-421. Menlo Park, California.

Ouimette, J. R. (1980) Ph.D. Thesis: Chapter 3 Application of Species Extinction Balance to Zilnez Mesa, Arizona. Calif. Inst. of Tech. Pasadena, California.

Ouimette, J. R., S. K. Friedlander, E. S. Macias, and P. H. McMurry (1980) Aerosol Chemical Species Contributions to Visibility Reduction in the Southwestern United States. Symposium on "Plumes and Visibility: Measurement and Model Components," Grand Canyon, Arizona, November 10-14.

Richards, L. W., J. A. Anderson, D. L. Blumenthal, A. A. Brandt, W. Jensen, W. S. Keifer, J. A. McDonald, J. L. Stith, and N. Waters (1980) VISTTA June-July 1979, Coal-Fired Power Plant Contribution to Visibility Impairment in Western Pristine Areas--Data Volume--MRI Airborne Sampling Data and Related Results from the June-July 1979 Field Program. MRI 80 DV-1717, Meteorology Research, Inc., Santa Rosa, California.

Richards, L. W., J. A. Anderson, D. L. Blumenthal, A. A. Brandt, W. S. Keifer, J. A. McDonald, L. R. Tanner, and N. Waters (1981a) VISTTA December 1979 Coal-Fired Power Plant Contribution to Visibility Impairment in Western Pristine Areas--Data Volume--MRI Airborne Sampling Data and Related Results from the December 1979 Field Program. MRI 80 DV-1783, Meteorology Research, Inc., Santa Rosa, California.

Richards, L. W., J. A. Anderson, D. L. Blumenthal, A. A. Brandt, J. A. McDonald, N. Waters, E. S. Macias, P. S. Bhardwaja (1981b) The Chemistry, Aerosol Physics, and Optical Properties of a Western Coal-Fired Power Plant Plume. Atmos. Environ. 15, 2111-2134.

Richards, L. W., G. R. Markowski, and N. Waters (1981c) Comparison of Nephelometer, Telephotometer, and Aerosol Data in the Southwest. Paper No. 81-54.5 presented at the Annual Meeting of the Air Pollution Control Association, Philadelphia, Pennsylvania, June 21-26.

Seigneur, C., R. W. Bergstrom, D. L. Blumenthal, L. W. Richards, E. S. Macias, W. E. Wilson, and P. S. Bhardwaja (1980) The Data Base for Visibility Model Evaluation from the June-July and December 1979 EPA-VISTTA Field Programs. Symposium on "Plumes and Visibility: Measurement and Model Components," Grand Canyon, Arizona, November 10-14.

Seigneur, C. (1982) A Model of Sulfate Aerosol Dynamics in Atmospheric Plumes. Atmos. Environ. 16, 2207-2228.

Sheppard, J. C., M. Campbell, P. H. McMurry, and G. L. Kok (1980) Trace Gas and Particle Data from a Remote Site in Northern Arizona. Unpublished results, Department of Chemical Engineering, Washington State University, Pullman, Washington.

Systems Applications, Inc. (1981a) Coal-Fired Power Plant Contribution to Visibility Impairment in Western Pristine Areas--Telephotometer Measurements--Data Sheets. Vols. I through IV, 339-ES81-11 to 339-ES81-14, Systems Applications, Inc., San Rafael, California.

Systems Applications, Inc. (1981b) Magnetic Tape with Telephotometer Measurements from the June-July and December 1979 VISTTA Field Programs. San Rafael, California.

Whitby, K. T. and G. M. Sverdrup (1978) California Aerosols: Their Physical and Chemical Characteristics. ACHEX Hutchinson Memorial Volume, Particle Technology Laboratory Publication No. 347. University of Minnesota, Minneapolis, Minnesota.

Wilson, J. C. and P. H. McMurry (1981) Aerosol Formation in Power Plant Plumes II. Secondary Aerosol Formation in the Navajo Power Plant Plume. Atmos. Environ. 15, 2329-2339.